Master of Science Thesis
HT2021

Surface Guided Helical Tomotherapy for Total Marrow Irradiation

Hedda Enocson

Supervisors

Sofie Ceberg, Per Engström, André Änghede Haraldsson, Malin Kügele, Jacob Engellau, Lund

π

Medical Radiation Physics, Lund
Faculty of Science
Lund University
www.msf.lu.se

Populärvetenskaplig sammanfattning

Leukemi kallas ibland blodcancer för att det drabbar de vita blodkropparna. I själva verket uppstår cancersjukdomen i de blodbildande organen, främst benmärgen och mjälten. Cellgiftsbehandling är den främsta behandlingstekniken men för patienter med hög risk för sjukdomsåterfall kan stamcellstransplantation vara aktuellt som del i behandlingen som ges i kombination med strålbehandling. Strålbehandlingens syfte är att slå ut resterande tumörceller efter cellgiftsbehandlingen samt hämma patientens immunförsvar så att de nya transplanterade stamcellerna kan etablera sig.

Strålbehandling är en viktig behandlingsmetod för cancersjukdomar och har som syfte att slå ut cancertumörer, bromsa cancersjukdom eller lindra symptom. Traditionellt har strålbehandling getts med statiska strålfält från olika vinklar inriktade mot tumörområdet. Ny teknik har möjliggjort dynamiska behandlingar där stråldosen levereras samtidigt som strålkällan roterar runt patienten och strålfältet kontinueligt formas efter tumörvolymen och anpassar intensiteten av strålfältet. Denna behandlingsteknik kan bespara närliggande friska organ från stråldos och dominerar strålbehandling idag. Strålbehandlingen planeras utifrån en skiktröntgenbild. Det kliniska målområdet för strålbehandlingen benämns CTV, clinical target volume. Denna volym omsluter den synbara tumören samt eventuella närliggande mikroskopiska maligniteter. Till CTV appliceras en marginal för att skapa volymen PTV, planning target volume. Genom att bestråla PTV säkerställer man tillräcklig dos till CTV. Storleken på marginalen beror på osäkerheter i CTVs position vid behandling. CTV och PTV utlinjeras av en läkare och överlämnas sedan till en dosplanerare som skapar behandlingsplanen. Planen optimeras så att dosen till PTV är tillräcklig medan dosen till riskorgan minimeras.

Strålbehandling inför stamcellstransplantation för högrisk leukemi har traditionellt getts som en TBI (total body irradiation) där hela patientens kropp behandlas för att nå målvolymen, benmärgen. TBI ges med statiska fält där hela patienten placeras i strålfältet. Ofta placeras blyblock framför lungorna för att minska dosen, men övriga riskorgan besparas inte. Behandlingen kan ge både akuta och sena biverkningar till organ som lungor, njurar, tarmar och linser. Ny teknik har möjliggjort en annan typ av behandling för leukemi, TMI (total marrow irradiation) där blodbildande organ och delar av kroppen där leukemiceller kan undkomma cytostatikaeffekter är målvolymen, främst benmärgen, och dosen till frisk vävnad kan minskas. Behandlingstekniken kallas helisk tomoterapi och skiljer sig från konventionell strålbehandling. Patienten ligger på en brits som sakta åker genom en maskin där strålkällan roterar kring patienten samtidigt som strålfältet formas efter målvolymen. Patienten bestrålas ett skikt i taget och strålen 'målar' ett helisk mönster av dos. Tomoterapi är fördelaktig för långa och komplicerade målvolymer och är därför en utmärkt teknik för TMI. Med TMI har man sett en minskning av biverkningar samtidigt som en lika god tumöreffekt kan bibehållas jämfört med TBI.

Vid varje behandlingstillfälle är det viktigt att patienten är positionerad likadant som när behandlingen planerades. För att åstakomma detta skapar man individuella fixationer som fästs i behandlingsbritsen. Fixationen kan bland annat bestå av en vacuumpåse gjuten för att följa patientens kropp och en mask för att hålla huvud och axlar på plats. Punkt tatueringar på patientens kropp och lasrar i rummet används för att positionera patienten på britsen. I behandlingsrummen har man dessutom ofta ett optiskt ytskanningssystem. Genom att projicera synligt ljus på patienten och detektera hur ljuset reflekteras kan man räkna ut en 3-dimensionell yta över patienten. Denna yta kan både användas som övervakning under behandlingen för att säkerställa att patienten inte rör sig men även för positionering av patienten. Genom att jämföra ytan med en referensyta från när behandlingen planerades kan patienten positioneras likadant vid varje behandlingstillfälle. Efter det att patienten positionerats tas ofta skiktröntgenbilder som jämförs med referensbilden för att verifiera patientens position. I detta examensarbete har positioneringen med optisk ytscanning utvärderats och jämförts med konventionell tatuerings positionering för patienter som genomgår TMI behandling. Resultatet har visar att ytskanning är ett användbart verktyg för att för att förbättra patient positioneringen. Med hjälp av ytscanningen kan osäkerheterna i patientpositioneringen reduceras, behandlings marginalen minskas och i sin tur stråldosen till frisk vävnad minimeras.

Abstract

Background: Total marrow irradiation (TMI) with helical tomotherapy treatment (HT-TMI) can be used as conditioning regimen for leukemia patients prior to stem cell transplantation by radiating the skeletal tissue. To ensure adequate dose coverage a margin is applied to the clinical target volume (CTV), i.e., planning target volume (PTV) margin. By applying as small margin as possible, the dose to organs at risk (OAR) is minimized. The PTV margin depends on the positioning deviation of the CTV. To aid accurate positioning, (on the couch prior to irradiation) an optical surface scanning system (OSS) can be used. By projecting visual light onto the patient surface and detecting the reflective light, the position of the patient can be calculated. The live surface is compared to a reference surface, i.e., the planned position, and any deviations can manually be corrected for. This application is called surface guided radiotherapy (SGRT).

Purpose: The purpose of this study was to investigate if SGRT, in comparison to 3-point localization, for HT-TMI can improve patient positioning and allow for smaller PTV margins that may reduce the dose to OARs.

Method and Material: A method was developed to position TMI patients using SGRT (Catalyst HD +, C-RAD, Positioning AB, Uppsala) on a Tomotherapy unit (Radixact, Accuray Inc., Madison, WI, USA). Four patients treated during October to December 2021 were included in the study. The patients were positioned using the developed surface guided method and the treatment margins were evaluated. The positioning deviations for the patients positioned using SGRT were retrospectively compared with the deviation observed for 16 TMI-patients previously treated and positioned using 3-point localization at another Tomotherapy unit (TomoTherapy, Accuray Inc., Madison, WI, USA). All patients were immobilized using full body vacuum bags and five-point open face mask and were treated with the same PTV margins. For both groups the margins were recalculated based on systematic and random set-up deviations measured from daily imaging. The target was divided into sub-CTVs for different body parts and treated separately when calculating the margin. The margin calculations were based on a population-based margin recipe derived by M. van Herk et al. 2000 to ensure a minimum dose to the CTV of 95% for 90% of the patients. The recipe was adjusted to be valid for treatments with few fractions. For the three patients positioned using SGRT, the calculated margins were evaluated by re-planning the treatment and comparing the dose to OARs. The reliability of the new margins was evaluated by recalculating the treatment plan onto the daily images and evaluating the 99.5% CTV dose coverage of the new plan in comparison to the original plan.

Result: The results imply that the positioning deviation decrease when using SGRT compared to conventional 3-point localization. The calculated margins were non-isotropic and could be decreased for skull, neck, thorax, pelvis and legs, however, kept the same for arms and increased in the vertical direction of the neck. When comparing treatment plans using the new margins with the original, the mean dose to OARs was reduced for the following organs: bladder, bowel bag, genitalia, heart, liver, kidneys, lungs, rectum. The median target coverage for $D_{99.5\%CTV}$ per fraction was 1.92 (range 1.81 – 1.94) Gy and 1.92 (range 1.71 – 1.94) Gy for the original plans and the new plans, respectively. In the $D_{99.5\%CTV}$ coverage no significant difference ($p<0.05$) was observed.

Conclusion: The developed method for Surface Guided Helical Tomotherapy for Total Marrow Irradiation can potentially improve patient positioning such that margins can be reduced which consecutively can reduce dose to OARs while maintaining target coverage.

Acknowledgement

I want to thank my supervisors for their time and effort in supporting me complete my master thesis. I have really enjoyed this semester and have learned from each and every one of you. To Sofie Ceberg, thank you for all the motivation and support, for being someone to bounce ideas with and for your positive attitude. Per Engström, thank you for sharing your knowledge and expertise in the TMI treatment and for the time spent troubleshooting and analyzing my results. Thank you Malin Kügele for sharing your experience in surface guidance and for your skill of keeping the project intriguing. To André Haraldsson, thank you for being the expert I needed in the tomotherapy system and for being there to discuss and reflect on all my ideas and questions. Thanks to Jacob Engellau for taking your time for all my questions and giving me insight of TMI from a medical point of view.

A special thanks also goes to all the tomotherapy treatment personnel for your faith and patient in me, making it possible to implement my study in the clinic. Thanks to the CT/immobilization personnel, Carola Hagström for taking the time in making TMI immobilizations for me. Thank you Marie Tärnhuvud for your support and sharing your knowledge in TMI - treatment planning. Finally, I want to thank the staff at the radiotherapy department and my peers for all the encouragement during countless coffee breaks.

Abbreviations

SCT - Stem cell transplant
RT - Radiotherapy
TBI - Total Body Irradiation
SSD - Skin-Source Distance
OAR - Organ At Risk
HT - Helical Tomotheraphy
TMI - Total Marrow Irradiation
CTV - Clinical Target Volume
CNS - Central nervous system
PTV - Planning Target Volume
IGRT - Image Guided Radiotherapy
CT - Computed Tomography
MVCT - Megavoltage CT
kVCT - Kilovoltage CT
SGRT - Surface Guided Radiotherapy
GVHD - Graft versus Host Disease
FOV - Field of View
CRD - Chronic Renal Disease
Linac - Linear accelerator
VMAT - Volumetric Modulated Arc Therapy
MLC - Multileaf Colimator
CT - Computed Tomography
OSS - Optical Surface Scanning
ROI - Region of Interest
DIBH - Deep Inhalation Breath Hold
HFS - Head first supine
FFS - Feet first supine
SUH - Skåne University Hospital
TPS - Treatment Planing System
FFF - Flattening filter free
FWHM - Full width half max
HU - Hounsfield units

Contents

1 Introduction

Leukemia is the collective name for cancer of the blood cells and includes several different diagnoses. The word leukemia comes from the Greek and means white blood, referring to cancer of the white blood cells. Approximately 700 people in Sweden are diagnosed with leukemia every year[1]. Leukemia is responsible for approximately a fourth of all cancers among children under 15. Treatment of leukemia almost always includes chemotherapy. The chemo can be combined with other medical treatments or with radiotherapy. The selected type of treatment depends on the diagnosis and the state of the patient. The goal of the treatment is to suppress all cancer cells, while doing so normal cells become deprived too. This causes the side effects with the treatment.

For high-risk leukemia eligible for stem cell transplantation (SCT) pre-transplant conditioning may include radiotherapy (RT). The traditional method of RT-deliverance before SCT has been as total body irradiation (TBI) [2]. TBI is often delivered with two conventional opposing fields, Anterior-Posterior and Posterior-Anterior. By using a large skin-source distance (SSD) the whole patient can be covered by the fields. The whole body is irradiated to cover the target, the blood forming organs, however, shielding of organs at risk (OAR) is limited. Therefore, the TBI treatment causes both acute and late side effects on the irradiated normal tissue. Most radiotherapy centers perform lung shielding for TBI [3][4]. This is to reduce lung toxicity and especially pneumonitis, radiation-induced inflammation of the lungs. In recent years helical tomotherapy (HT) has shown to be feasible for total marrow irradiation (TMI) which allows for a reduced dose to OARs such as lungs, kidneys, bowel bag among others [5]. With the helical tomotherapy technique treatment can be conformed around the clinical target volume (CTV) which entails the bone marrow compartment, the spleen, and for some leukemia subtypes also the central nervous system (CNS) and testicles. With HT, this is achieved by irradiating the patient one slice at the time as the patient translates through the modulated radiation fields, similar to computed tomography (CT). HT, in comparison to the more common volumetric modulated arc-therapy (VMAT) technique, allows to treat long and complicated targets. This makes HT an eminent option for TMI where the treatment can be delivered by at most dividing the target into two parts. The conform technique require accurate patient positioning. A margin is added to the CTV to create the planning target volume (PTV). By irradiating the PTV, adequate dosage to the CTV is ensured. The size of the margin can be determined based on positioning errors [6]. To verify the position, image guided radiotherapy (IGRT) using either megavoltage CT (MVCT) or kilovoltage CT (kVCT) is used. Such IGRT and especially MVCT, is both time consuming and contribute to additional dose to the patient. A good pre-positioning is warranted to prevent re-positioning and additional imaging. To achieve this, an individually molded immobilization is used. Traditionally, the patient is then positioned using 3-point localization with tattoo markers and lasers. To further improve patient pre-positioning surface guided radiotherapy (SGRT) is used. SGRT systems project optical light onto an object and calculate a 3D surface by detecting the reflected light with optical triangulation. A SGRT system with a large field of view (FOV) has been implemented in the clinic to enable positioning of large targets such as for TMI.

The aim of this master thesis was to investigate if SGRT, in comparison to 3-point localization, for HT-TMI can improve patient positioning and allow for smaller PTV margins that may reduce the dose to OARs.

2 Background

2.1 Leukemia

Leukemia is cancer of the body's blood-forming tissues, including the bone marrow and/or the lymphatic system. When the cancer cells in the bone marrow multiply the production of normal blood cells becomes suppressed. The lack of normal blood cells causes the symptoms of fatigue, fever, infections, weight loss, skeletal pain and swollen lymph nodes and spleen. Leukemia is divided into two categories, chronic and acute. Chronic leukemia occurs most often in older adults while acute leukemia occurs in all ages. Both acute and chronic leukemia is divided into lymphocytic and myeloid. Acute lymphocytic leukemia is the most common type among children. Leukemia can be diagnosed with a blood test and the type of leukemia can be determined with a bone marrow sample. The treatment of leukemia includes chemotherapy and is sometimes combined with other medicinal treatments or radiotherapy. In some cases, the final step of the treatment includes a stem cell transplant to replace the deprived bone marrow. The stem cell transplant can be autolog, extracted from the patient's own blood or bone marrow or allogen, from a donor [1]. The treatment before the transplant is described as conditioning regimen. The goal of the conditioning regimen is to suppress the immune system so that the patient will not reject the new bone marrow, make room in the bone marrow for the donor marrow stem cells to grow and destroy cancer cells [7].

Graft versus host disease (GvHD) is a condition that might occur after an allogeneic transplant. In GvHD, the immune cells in the transplanted tissue view the recipient's body as foreign and attack the recipient's tissue. GVHD is divided into acute and chronic, where acute GVHD occurs within 100 days after transplantation and chronic occur up to a year after transplantation. Acute GVHD increase the risk of chronic GVHD. The stem cell donor can be a related matched donor or an unrelated matched donor. A related donor is shown to give a higher success rate in terms of GVHD- free survival. GVHD complications are typically dermatitis (skin inflammation), hepatitis (liver inflammation), enteritis (bowel inflammation), diarrhea and vomiting. Overall, about 40% of leukemia patients that undergo stem cell transplant die from GVHD complications or relapse.[5]

Aside from GVHD, there are side effects associated with the radiotherapy. There are acute and late toxicities that depend on the irradiated volume and the level of shielding of OARs. After TBI conditioning, acute toxicities that can be expected include parotitis (inflammation of the parotid glands), xerostomia (impaired salivary gland function), mucositis (inflamed mucous membrane usually in mouth, esophagus and bowel), skin erythema, headache, hair loss, nausea, vomiting, diarrhea, loss of appetite, and fatigue [8]. These effects occur days or weeks after the RT. With TMI the dose is conform around the target volume and the dose to normal tissue and OARs is reduced. Due to this a low occurrence of acute toxicity has been seen [9]. After RT, late effect may include interstitial pneumonitis, chronic renal disease (CRD) and lens cataract [10] [11]. The occurrence is reduced with reduced dose. Children suffer more profound late effects [12] [13]. Late toxicities in children may include negative effects on cognitive processes, growth, and endocrine and metabolic functioning [12] [13].

2.2 Helical Tomotherapy

External radiotherapy plays an important role in cancer treatment. Depending on the diagnosis of the patient and the purpose of the treatment, the treatment is divided into one or several fractions. The dose is administrated using linear accelerators (linac). In the most common type of RT the linac is mounted

on a gantry on a C-shaped arm. The patient is mostly immobilized on a couch in a fixed position. The dose is delivered in either stationary fields with the gantry in different angels (conventional radiotherapy) or while the linac is rotating around the patient with continuously reshaping fields (Volumetric Modulated Arc Therapy, VMAT). The dose is conformed and intensity modulated to the target using multileaf collimators (MLC).

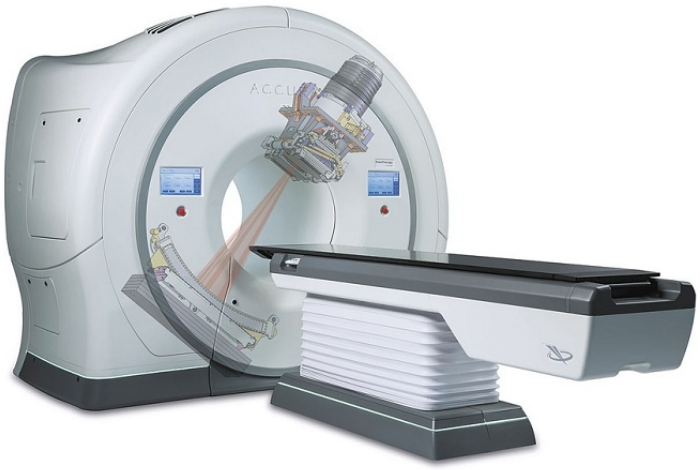

Figure 1: *Tomotherapy unit produced by Accuray [37].*

In helical tomotherapy a different technique is used. The technique is based on the same principle as a computed tomography (CT) but with higher photon energy and dose rate. The linac is mounted in a slip-ring, enclosed in a bore. The gantry can rotate relatively quickly around the patient with a rotation speed from 11.8 to 60 s. The patient is irradiated one slice at the time as the couch moves across the rotating strip beam. The linac rotates around and is radiating the patient continuously as the couch moves through the bore, creating a helical trace of the beam. The perks of this technique in comparison to conventional radio therapy is that it allows treatment of very long and complicated targets. With current tomotherapy machines, targets up to 135 cm can be treated with HT. A collimator pair determine the width of the strip beam. The beam is modulated to the target using binary MLC. The 64-leaf MLC open in the longitudinal direction. They can open and close in approximately 20 ms and affect the beam latency. The linac is close to the MLC bank, therefor, the beam output from one MLC leaf depends on the number of open adjacent leaves. The speed of the couch and the gantry rotation are defined by the planning parameters pitch and modulation factor. The modulation factor MF is defined as the ratio between the MLC's maximum and mean opening time and is used to adjust the level of intensity modulation to obtain a homogeneous and conform dose distribution. The pitch P is defined as the fraction of the distance the couch travels per rotation and the beam width. The tomotherapy unit is equipped with imaging devices for image guided radio therapy (IGRT). By scanning the patient before treatment, the position of the patient can be verified using the reference CT. The treatment machines used in this study are TomoTherapy HD and Radixact, both produced by Accuray (Figure 1). For the treatments studied in this report the maximum delivery rate is 860 cGy/min at 1.5 cm depth. The TomoTherapy is fitted with an MVCT for IGRT. The Radixact is based on the same concept as the TomoTherapy but can deliver a higher dose rate and has a couch catcher that prevents the couch from sagging when the couch travels through the bore. The couch sag is a known default in the TomoTherapy. The Radixact is equipped with kVCT which enables a faster imaging with a wider FOV and better quality images [5].

After automatically or manually matching the verification image with the reference CT, the position error is obtained in 6 degrees of freedom, three translations and three rotations. The translation (lat, long and vert) and rotation (roll, pitch and yaw) directions are illustrated in Figure 2. Before treatment the couch

is corrected according to the position error. The rotational errors yaw and pitch has to be corrected by manually moving the patient. Roll can be corrected automatically in the machine by adjusting the starting angle of the treatment [5].

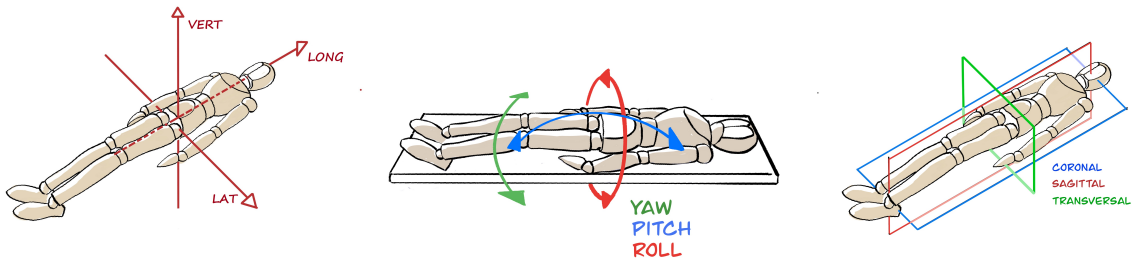

Figure 2: *Explanation of translation directions, rotation around the different axis and viewing planes. Illustrations by Per E. Engström.*

The helical technique can be applied to many types of targets. Targets treated with HT at Skåne University Hospital are typically cancers of the head and neck, thorax, abdomen or pelvic area [14]. TMI for leukemia patients and total skin irradiation (TSI) for patients with mycosis fungoides (that generally affect the skin with tumors) are examples of large and complicated targets. These treatments have been shown to benefit from HT [9] [15].

2.3 Optical Surface Scanning

Optical surface scanning (OSS) is a tool that can provide information of the patient setup without contributing any radiation exposure to the patient. There are several techniques for optical surface scanning. The basic concept is to project optical light on the surface and to detect the reflected light using one or several 3D camera units. The surface is calculated using optical triangulation. The main techniques today are laser scanners, time-of-flight systems, stereovision systems and structured light systems. All systems use a absolute coordinate system that is calibrated to treatment iso-center. The OSS used in this study is a structured light system called Catalyst HD+ (C-rad Positioning AB, Uppsala Sweden). Catalyst use a grid to calculate the position of a discrete number of points in the surface. Structured light systems project a light with a known pattern onto the object. When the reflected light gets detected by the camera it has been distorted by the shape of the surface of the object. By comparing the projected and reflected pattern the position of each point in the surface grid can be calculated (Figure 3)[16].

A reference surface is either obtained using the OSS system during the reference CT scan or from outlining the body of the patient in the reference CT and exporting this structure to the OSS system. The reference surface is then matched with the live surface from the treatment session. The two surfaces are matched using rigid or deformable registration. The surface is defined as a grid of discrete points. In rigid registration these points are matched with the reference surface with a "closest neighbor" method. All points in the two surfaces are included in the registration. A ROI (region of interest) can also be applied in rigid registration where the points in the ROI are given a higher weight to be of more significant in the match. The ROI is chosen by the user and is typically set to rigid structures with respect to the target such as bone structures. A downside to this is that the match will depend on the judgement of the user when defining the ROI.

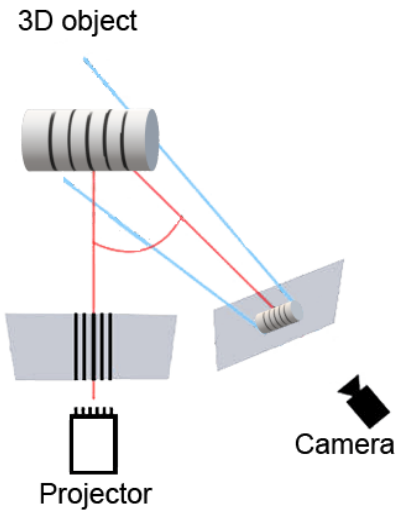

Figure 3: *Principle of a structured light system. Structured light projected onto a 3D object, reflected and detected by a camera. The projector and the camera are positioned at an angel (red lines) and the surface is calculated with optical triangulation. The blue line represents the FOV of the camera.*

Rigid registration is also sensitive to deformations in the live surface that does not necessarily affect the target position. Surface deformations can be due to swelling or weight loss, common side effects during cancer treatment. In rigid registration, deformations may lead to the system failing to match the two surfaces [16]. The OSS used in this study use a deformable image registration. The deformable registration starts by aligning the live surface with the reference surface based on a rigid registration. From this a similarity index is calculated. The deformable registration algorithm then tries to maximize the similarity. In the registration a similarity index is calculated based on all the points in the two surfaces where the points near the iso-center are weighted higher. The optimization is an iterative process where deformations are identified to alter the live surface. The deformed live image is then once again compared to the reference image for a number of iterations until a given similarity index is achieved. The process is non-linear in the sense that the algorithm tires to identify local max and minimums in the surface and the surface points close to the treatment iso-centre are assigned higher weight in the registration [17]. The deformations found in the registration are back projected onto the patient skin in the form of a color map. This gives the Radiation Therapist live feedback on the patient's posture. The registration finally returns the calculated iso-center position in 6 degrees of freedom. S. Pallottaa and M. Kügele et. al. found that deformable image registration compared to rigid registration in OSS significantly improved positioning accuracy in the lateral and longitudinal directions and in pitch when studying a deformable phantom [18].

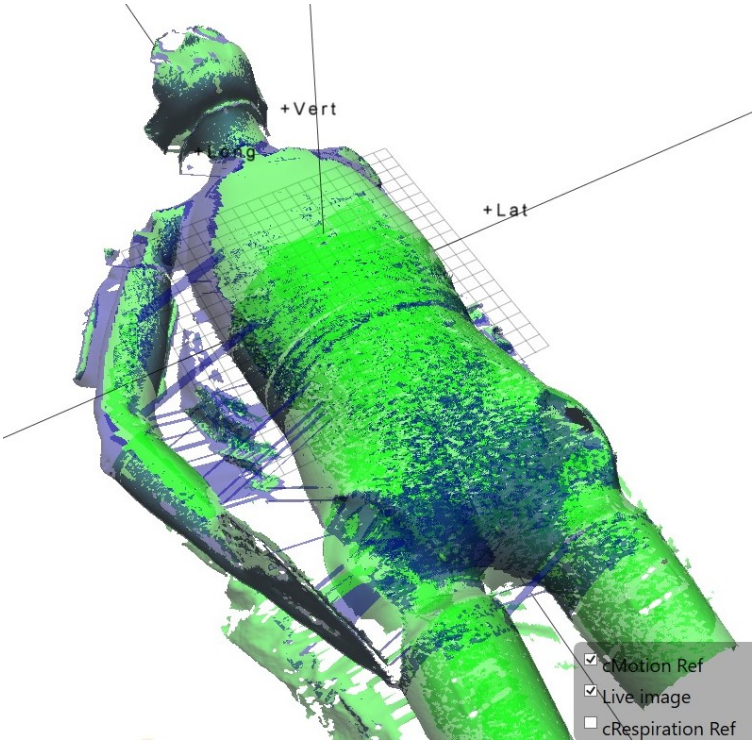

Figure 4: *Live (green) and reference (blue) surface of a whole body phantom positioned with the OSS system Catalyst HD+ (C-rad).*

Once the registration is made the patients posture is corrected. The three translations are corrected by shifting the couch in lat, long and vert direction. The rotations roll, pitch and yaw need to be corrected manually. In this step the color map is of help to find which direction to rotate the patient. The color map projects yellow in regions where the live surface is below the reference surface and red where the live surface is above the reference surface. If the live surface is within a chosen tolerance with respect to the reference surface the color map is green, and no light is projected onto the patient. Deformations such as incorrectly positioned arms can also be corrected using the color map. Once the patient is corrected and the errors are within a defined limit the patient can proceed to treatment. Figure 4 shows a phantom positioned with OSS system. M. Kügele and A. Mannerberg et. al. have showed that OSS improves positioning of patients compared to three point localization markers with room lasers [19] [20]. The three-dimensional (3D) average displacement vector v is calculated from individual displacement in x, y, and z directions using,

$$v = \sqrt{x^2 + y^2 + z^2}. \tag{1}$$

For prostate cancer patients receiving ultra-hypofractionated radiotherapy the median vector offset v was found to be 4.7 mm (range:0 – 10.4 mm) for OSS and 5.2 mm for 3-point localization (range: 0.41 – 17.3 mm)[20]. They also found that the median setup time could be decreases using OSS from 3:28 min for 3-point localization to 2:50 min. For breast cancers patients receiving tangential treatment it was found that 95% of the treatment sessions were within the clinical tolerance of $\leq$ 4mm in any direction using OSS, compared to 84% for 3-point localization. For patients receiving locoregional treatment 70% and 54% were within the tolerance for OSS and 3-point localization, respectively[19].

During treatment the OSS offer motion management to ensure that the patient lies still during beam on time. The OSS is connected to the linac such that if the patient's movement exceeds a defined limit the beam is rapidly switched off. Catalyst also offers gating guidance in deep inhalation breath hold (DIBH). DIBH can be used for treatment of breast cancer, Hodkin's lymphoma among other treatment sites. By only treating the patient in DIBH OARs can be spared. This is frequently used on left sided breast cancer to spare dose to the heart. When delivering a gated treatment, the OSS tracks the movement of the thorax and enables the beam to be on only when the thorax is in a position window when the patient holds their breath. When the patient moves in- and out-side of this window the beam is turned on and off. To ensure correct dosage the

beam needs to be turned off rapidly if the patient moves outside of the tolerance. To do this the communication between the OSS and the linac is essential but the latency time also depend on how fast the linac can stop the beam. M. Lempart and M. Kügele et. al. have studied latency characterization of gated radiotherapy treatment beams [21]. Their results of beam-off latency were in the order of 57 (60) ms and was considered sufficient based on the tolerance of 100 ms recommended by the American Association of Physics in Medicine.

The OSS system Catalyst HD+ (C-rad Positioning AB, Uppsala Sweden) is a three-camera system that is currently installed at the helical tomotherapy units used in this study. Each camera can cover a FOV of $1100\times1400\times2400$ mm^3[22]. With this FOV, a three camera system can cover a whole body, which makes it suitable for positioning patients with long targets. This feature is favourable for many HT treatments and for TMI in particular. As the couch translates through the bore the OSS can follow the couch and enable motion management during treatment. This function is not yet implemented clinically at Skåne University Hospital (SUH) and is not used in the treatments studied in this report. The TomoTherapy machine at SUH was previously equipped with a different OSS system, Sentinel (C-RAD Positioning AB, Uppsala, Sweden). A. Haraldsson et. al. have in a study presented the difference in positioning errors at the TomoTherapy between surface guided and three-point laser based setup [14]. The study was based on 894 HT treatments where 16 835 fractions were evaluated based on the MVCT images. For all treatment sites (CNS, head and neck, thorax and abdomen) they found that the correction vector v was significantly smaller for those fractions positioned with OSS. From this they concluded that, for the current margins, a weekly MVCT was sufficient in combination with SGRT. By implementing this they also found that the patient on-couch time could be significantly reduced for all treatment sites. The time-reduction was both due to the long image acquisition time of the MVCT and the time it takes to evaluate the image.

For treatments without daily imaging, OSS systems can function as IGRT without contributing to extra imaging dose or on-couch-time for the patient. For treatment fractions where imaging is required the OSS system can warrant a better pre-position and minimize the risk of needing to re-position the patient after evaluation the acquired image. The system also offers real-time surveillance during the treatment that ensures that the patient does not move during the treatment.

2.4 Total marrow irradiation

In total marrow irradiation the red bone marrow is the target but the whole skeletal tissue is outlined as the CTV. With this, the CTV includes a margin depending on the thickness of the cortical bone. The thickness on the cortical bone varies through the different bones but also depend on gender and age. In addition, brain, spleen, lymph nodes and testes are sometimes included as target depending on the patient's diagnosis. Cartilage and skeletal structures lacking red marrow are excluded from the CTV. The target is as long as the patient. For adults this means that the target needs to be divided into two treatments to not exceed the maximum HT target length of 135 cm. The patient is CT-scanned in two parts, in head first supine (HFS) position to cover the upper body and in feet first supine (FFS) position to cover the legs. The two scans combine in a junction on the upper thigh. This junction is a crucial location when planning and delivering the treatment to make sure no part of the target gets under- or overdosed. To ensure robust dosage over the junction each treatment is planned with a sloping dose level where the treatments overlap. By applying a dose gradient in opposite directions for the two plans under-and over- dosage will be minimized in case of positioning errors in the longitudinal direction [23]. The junction dose is illustrated in Figure 5. The

margin is calculated based on setup errors that are both systematic and random. When calculating the margin around the CTV, a common aim is to create the PTV such that for 90% of the patient population, the minimum dose to the CTV is 95% or more of the prescribed dose [6]. Since the errors deviate between the different skeletal structures the margin is not uniform over the whole target [23].

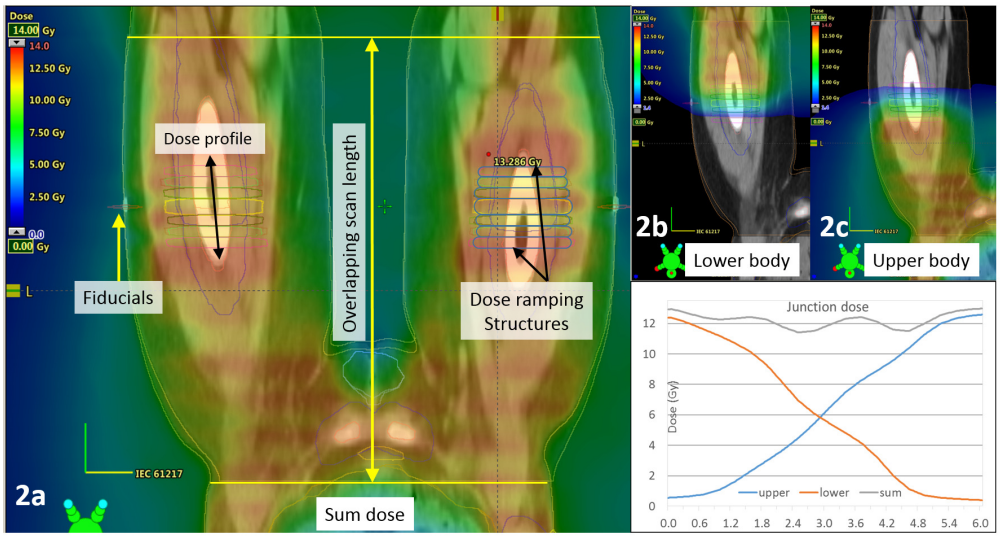

Figure 5: *Coronal plane of junction on upper thigh. Dose profile over the junction for the two plans along with the sum of both plans [23]* .

In a study by A. Haraldsson et. al total marrow irradiation was compared to total body irradiation prior to allogeneic stem cell transplantation [9]. The study was a prospective analysis of 37 patients receiving TMI and compared with 33 consecutive previous patients receiving TBI prior to SCT. The patients receiving TMI were irradiated with a helical treatment at the TomoTherapy HD. The prescribed dose was 2 Gy/fraction with a total dose of 12 Gy for all patients. The TBI patients were treated with a conventional technique at a 4,5 m distance from the radiation source and a maximum absorbed dose rate of 30 cGy/min 1.5 cm depth. The occurrence of graft-versus-host disease and relapse after TMI and TBI was compared in the study. The rate of engraftment, when the bone marrow starts to produce blood cells after the transplant, was also compared. The results showed that the 1-year graft-versus-host and relapse -free survival was significantly higher for patients treated with TMI. Treatment related toxicities were of low occurrence in the TMI cohort. This strengthens the impression that conditioning with TMI generally results in a lower occurrence of toxicity, treatment-related mortality and GvHD. The results also showed that the time for engraftment with a platelet count over 20 [K/µL] and 50 [K/µL] was significantly shorter for the TMI group. The engraftment of neutrophil did not show any significant difference between the two cohorts. This is in agreement of previous trials where dose distribution and dose rate correlate with engraftment. With TMI in comparison to TBI the mean dose to several OARs is reduced but the integral dose is also reduced. The integral dose is the product of mass of irradiated tissue and absorbed dose. Generally it is accepted that the risk of normal tissue complication and secondary malignancies increase with increased integral dose, however, the integral dose is normally not used when evaluating treatment plans [24].

2.4.1 TMI protocol, Skåne Univerity hospital

The treatment procedure for TMI treatment at Skåne Univerity Hospital is explained below [25]. A study on implementing safe and robust Total Marrow Irradiation using Helical Tomotherapy by A. Haraldsson et.

al has given the scientific foundation to support this protocol [23].

The most common prescription for TMI at SUH is 12 Gy given in 2 Gy per fraction in 6 fractions twice daily. Older patients are given 10 Gy over 5 fractions to minimize the risk of severe complications. There are different protocols on how the fractions are distributed. Pediatric patients, and occasionally adults, are typically given two fractions per day Wednesday- Friday with at least 6 h between each fraction. The radiotherapy is then followed by chemotherapy. Adults are often treated with chemotherapy before radiotherapy and receive one fraction in the afternoon of the first day then two fractions per day and one fraction in the morning of the last day. The treatment is then followed by stem cell transplantation in the afternoon.

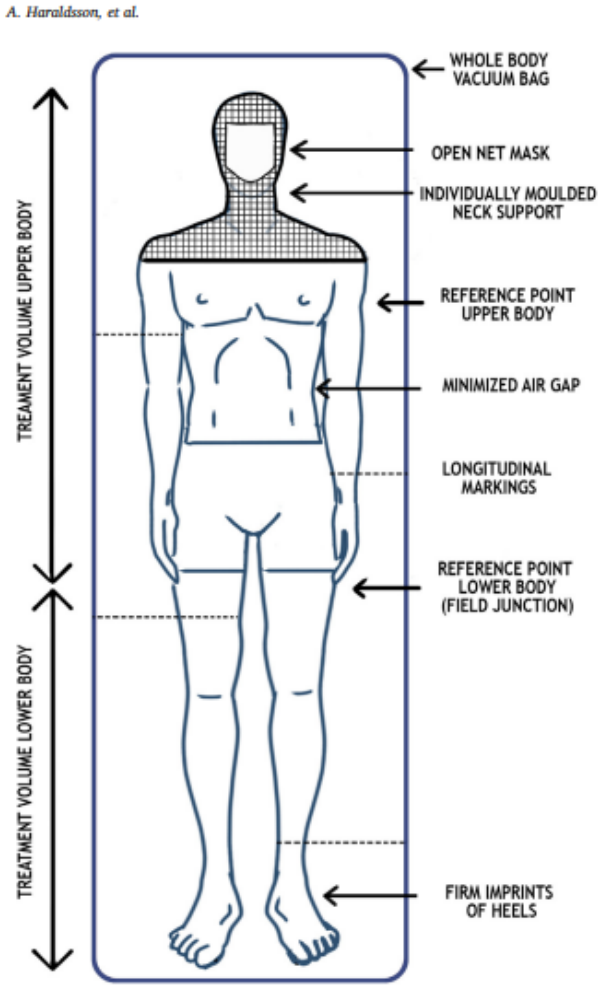

Figure 6: *Illustration of the patient immobilization equipment and reference points. Illustration by Per E. Engström.*

The immobilization includes the following (Figure 6). An individually molded headrest (Mouldcare RI II-HN, RT-4492) with different sizes if the patient is adult or a child. A high precision base plate in Carbon Fibre Low Density (Art. No 32110) that secures a five-point Hydbid Open face Mask (HP Eff 1.6 mm micro, Nano 1.2 mm micro) and holds the patients head, neck and shoulders. An individually molded full body vacuum bag (Vac Fix vacuum bag) with a styrofoam (half cylinder) under the bag for knee support. The bag is placed on the mask base plate that creates an indent on the backside of the bag. This way the bag can be placed on the same place with respect to the head and shoulder immobilization every time. The patient is placed flat and straight on the bag. The bag is molded to follow the body and embrace the arms, legs and feet. The legs are placed stretched out with a small distance between. The heals and sides of the feet are molded in the bag with the toes free. Under the bag is a carbon fiber rail with a fixation puck placed and molded into the bag to immobilize the bag in the lateral direction. During the immobilization it is important to make sure the patient has free airways and lies comfortable since the TMI treatment time is long. If the immobilization is putting pressure against the patient's skin, compresses are placed to reduce discomfort and the risk of wounds. The patient is then immobilized on a CT unit couch and scanned in two parts. To verify that the fixation is straight, lines are drawn on the bag and, on the mask, using lasers in the room. The upper body is scanned first. The patient is placed in HFS position. With help from the in-room lasers the patient is tattooed at the inner reference point on the thorax and at the junction on the upper legs. Glass CT-markers are taped in these points and on top of the thighs to mark the transverse position. Several lines are also drawn on the patient and the bag to mark the position. The patient is

then scanned from the top of the head to approximately 10-20 cm below the junction markers. A FOV of 500-650 mm is used and a slice thickness of 5mm. The immobilization is then rotated 180 degrees and the patient is positioned FFS and aligned with the lasers and tattoo markers. An additional lead marker is placed between the legs to mark the sagittal position. The body is scanned from the feet till the middle of the pelvis with FOV 500 mm and slice thickness 5 mm. Both the HFS and FFS position is documented with pictures. During the scan the patient is instructed to breath calmly. The images are exported to the treatment planning system (TPS).

The structures are outlined in Eclipse Contouring. The CTV is drawn in separate structures; head with the CNS included depending on the diagnosis, body and the spleen with the arms excluded, lymph nodes and testis included depending on diagnosis, right arm, left arm, right leg, left leg. On the thorax the ribs are merged to one continuous volume and the ventral cartilage is excluded. The toes, fingers, sesamoid bone, hyoid bone, larynx and kneecap are excluded from the CTV. From each CTV a margin is added to create the PTV structures. For PTV(head) 7 mm margin is added, PTV(body-arms) 10 mm is added, for young patients shorter than 160 cm generally a margin of 8 mm is added to minimize the dose to OARs, PTV(arms) 10-15 mm and PTV(legs) 10 mm. For superficial CTVs these margins may result in a PTV outside of the surface of the patient. In this case an optimization bolus of density 0.6 kg/m^3 is applied to avoid optimization in air. If the dose distribution is optimized in air, without a bolus, it may result in over-dosage at the surface due to positioning uncertainties during treatment. Optimizing the dose distribution with a bolus set to the density of tissue (water) would cause a smaller over-dosage since the bolus is not actually there during treatment. Density 0.6 is a compromise between the two scenarios. The following OARs are also outlined; lungs, kidneys, bowel bag, heart, brain, lens, eyes, parotis, submandibular gland, oral cavity, thyroid, larynx, esophagus, stomach, pancreas, spleen, liver, breast, genitalia, rectum, Port-a-cath. The OARs are outlined to report the dose level but only lungs, kidneys, heart, bowel bag, genitalia and liver are prioritized in the dose optimization. A structure outlining the body is also created. To create a robust dose plan in the junction between the two plans each plan is created to have a dose fall of 2 Gy/cm with opposing direction of the dose fall-off gradient. The junction lies in the middle of each plans dose gradient. To do this, 6 additional structures are drawn around the PTV with a margin of 0,5-1 cm. This additional margin is to ensure a robust distribution in the junction. Each structure extends over two image slices to have a length of 1 cm. The dose distribution is then created in two plans, for the thorax and the legs in Accuray's TPS Precision. The energy of the photons is 6 MV and the dose rate is 1180 MU/min. The structures in the junctions with each dose criteria are prioritized first during the optimization, then the different PTVs are prioritized and finally the dose to the OARS are minimized in the order as listed above. The TPS user sometimes create help structures to push the distribution in the desired directions. Typically, the thorax plan is made first. Once the leg plan is finished the two images and dose distributions are matched with the junction markers to create a summarized plan. This visualizes the distribution over the junction. The two plans use the same pitch of 0.397 and the modulation factor is set between 2.5-2.8 for the upper body and 1.6 for the lower body. The optimization is done in at least 400 iterations and the final plan should have a beam on time of 0.12-0.13 minutes/cm body length to prevent too long treatment times. In the treatment plane the 95% iso-dose surface covers most parts of the CTV and the 93% iso-dose surface should completely enclose the CTV. The outlined body structure is exported to the OSS system. In the OSS system the abdomen is cropped out from the reference surface to reduce the impact of swelling or weight loss.

During treatment a black sheet is placed over vacuum bag before the patients lies down to minimize reflections from the immobilization in the SGRT registration. The thorax is treated first. The patient is

positioned using the tattoo points, the drawn lines and the in-room lasers. The junction tattoos on the thighs are marked with lead markers. The OSS system is used to adjust the position of the arms and legs, but the suggested couch shift is ignored. During the first two or three fractions an MVCT or kVCT, depending on treatment machine, is acquired. After the image is matched the position is adjusted in lat, long and vert direction as well as roll. Other rotational errors must be adjusted manually and may require and extra image. The longitudinal match should be within 5mm of the junction markers and still have a good match on the head. After the upper body has been treated the patient gets a short break while the immobilization is rotated. The image match on the legs should not deviate from the junction markers to ensure a adequate dose coverage in the junction. In case of a good positioning result from the verification image, deviations less than 3mm in any direction, the following treatment fractions can proceed without CT imaging and with only OSS as image guidance.

2.5 Margins and errors in radiotherapy

In radiotherapy there are several errors that may make the prescribed dose differ from the delivered dose. To make sure the dose to the CTV is sufficient a margin around the CTV is added to create the PTV. A common criteria for the margin is to ensure that for 90% of a patient population, the minimum dose to the CTV must be 95% of the prescribed dose or higher. The margin for a treatment is derived from errors that are random and systematic. Gross errors that should be caught with quality assurance are not included in the calculation of the margin [6]. It is assumed that by finding the smallest margin around the CTV, that fulfill the criteria, the damage to OARs is minimized. Therefore OARs are not taken into account when calculating the margin [26]. Random errors lead to a blurring of the dose distribution and systematic errors lead to a shift in the dose distribution with respect to the prescribed dose distribution [26]. The following calculation of the errors and margins is based on a derivation by M. Herk et. al. [26]. In the computation each part of the CTV is considered equally important and is based on the probability density of the dose delivered to the CTV. In short, the derivation includes the convolution of the dose distribution and the random errors to estimate the cumulative blurred dose distribution. Next this blurred distribution is shifted by the systematic error and analyzed within CTV. Finally, the probability distribution of the systematic errors is used to compute what percentage of a group of patients receives a certain dose distribution.

The first errors occur during the scan of the reference images used for treatment planning. When the scan is made the patient needs to be positioned relative to the origin of the scanner equipment using lasers and tattoo marks on the patient. This setup procedure will involve an error s_0. The obtained image is a snapshot in time of moving organs and will cause a second error. In the image the CTV and other organs are frozen in time in a position. The CTV frozen position $M(0)$ in the image does not correspond to the position of the CTV at all times. To investigate the magnitude of the organ motion error a 4D-CT can be acquired to visualise the target position over a breath cycle. When delineating the CTV a third error d is introduced[26]. The error is based on how one observer delineates compared to another, but there are also differences if one observer is asked to delineate the same CTV twice [6]. The magnitude of this error depend of the location and tissue of the target but also on the imaging modality [27]. For prostate cancers the magnitude of delineation errors have been reported to be between 2-3 mm standard deviation [28]. For other cancer sites such as breasts the error have been reported to be of greater magnitude mainly depending on the experience of the radiation oncologists [29]. Some targets can be defined with automated segmentation when the density of the target is separated from the density of the surrounding tissue. This has been reported to give a good delineation accuracy for skeletal tissue in CT images [30] and brain structures in MRI images

[31]. Automated segmentation also significantly reduces the delineation time. The outlined position of the CTV is given by,

$$x_{delineated} = M(0) + s_0 + d \tag{2}$$

The terms $M(0)$, s_0 and d are all contributing to systematic errors, they will affect each fraction of the treatment the same amount and in the same way. However, the errors are stochastic over a treatment group of patients and for different scans. The variance in each systematic error is written as $\sum_m^2$, $\sum_s^2$ and $\sum_d^2$. The delineated CTV will then be the main objective when planning the treatment. The planned dose distribution can be written as.

$$D_{planned}(x) = D(x - x_{delineated}) \tag{3}$$

where $D(x)$ is the ideal dose distribution according to the prescription. During the treatment fractions the CTV will move with respect to the planned dose distribution due to setup error and organ motion. These errors are both random and systematic. The random errors will cause a blurring of the dose distribution $D_{blurred}$. In this derivation errors due to CTV distortion are ignored and all errors are explained in terms of translation. The variances of organ motion and setup error during treatment that cause the blurring of the dose are written as σ_m^2 and σ_s^2. For a CTV with a 1D, 2D or 3D distribution the cumulative dose distribution can be written as,

$$D_{cum} = D_{blurred}(y - x_{delinated}) \tag{4}$$

where y is the position in the CTV relative to a reference point e.g. center of mass in the CTV. D_{cum} is a shifted version of $D(x)$ due to systematic errors that has been blurred due to random errors. C is the collection of $x_{delineated}$ in which $D_{blurred}$ exceeds a threshold value $D_{threshold}$.For $D_{threshold}$ of 95% C holds the volume of the 95% isodose surface of $D_{blurred}$. If $D_{threshold}$ should exceed the minimum dose in the CTV, C is written as,

$$C : \left\{ x_{delineated} \middle| \min_{y \in CTV} D_{blurred}(y - x_{delineated}) > D_{threshold} \right\} \tag{5}$$

where y is an "integration variable" that is used to search for the minimum dose in the CTV. The probability P that the cumulative dose to the CTV exceeds this threshold for a group of patients is given by,

$$P(D_{cum} > D_{threshold}) =_C Q(z)dz \tag{6}$$

where Q is the probability density of the systematic errors and can be written as $Q(z) = G(z, \Sigma^2)$. G is assumed to be Gaussian and $\Sigma^2 = \Sigma_m^2 + \Sigma_s^2 + \Sigma_d^2$ is the combined variance in all systematic errors (motion, setup and delineation).

By reversing the computation, margins can be derived. First the collection C in equation (5) is set to a volume of radius $\alpha\Sigma$. Since the variance of the systematic errors is not necessarily the same in all directions, Σ is a 3D vector. Next the probability that the systematic errors belong to C for a group of patients is set to the desired value in equation (6). M. Herk states that in a 3D volume for a probability of 90% α is 2.5. Next an extra margin must be chosen to account for random errors. This margin depend on the chosen $D_{threshold}$. For $D_{threshold} = 95\%$ the extra margin is the distance between the 95% isodose surface of $D_{blurred}$ and $D_{planned}$. By taking the 50% isodose surface as reference since it does not shift due to blurring the extra margin can be written as $\beta\sigma - \beta\sigma_p$. $\beta\sigma$ is the distance between the isodose surface of 50% and 95% in $D_{blurred}$ and $\beta\sigma_p$ is the same distance in $D_{planned}$. σ is the combined variations in random errors (setup and motion) and can be written as $\sigma^2 = \sigma_m^2 + \sigma_s^2 + \sigma_p^2$. σ_p is the standard deviation that describe the

width of the penumbra in the dose distribution. σ and σ_p are vectors and allows to calculate non-isotropic margins. M. Herk derives the numerical value of β, for the 95% isodose surface β =1.64. The margin can be written as,

$$m_{PTV} = \alpha\Sigma + \beta\sigma - \beta\sigma_p. \tag{7}$$

To simplify equation (7) the penumbra with can be excluded and the margin can be written as,

$$m_{PTV} = \alpha\Sigma + \gamma\sigma' \tag{8}$$

where $\sigma' = \sqrt{\sigma_m^2 + \sigma_s^2}$. γ depend on the penumbra width and the rage of uncertainty. M. Herk computes γ to be 0.7 for a 95% dose level and a penumbra width of 3.2 mm [26].

For RT with conventional fields the penumbra width can be estimated from a dose profile. With VMAT the dose is not delivered in static fields. Therefore, it is difficult to define the penumbra since the dose is optimized to be conformed around the target. The definition of penumbra width is also flawed for flattening filter free (FFF) treatment techniques since the dose profile is never flat. This limitation of the margin formula may lead inaccuracies depending on the shape of the penumbra and the dose profile, on the conformity of the treatment, the density of the target and sounding tissues and the treatment technique [32]. G. Ecclestone et. al. have calculated the penumbra width for VMAT to the lung tissue to be 6.4 mm [32]. M. Groher suggests a penumbra width of 5 mm when evaluating the PTV margin of prostate cancers treated with either VMAT or 13-feild step and shoot [33]. In these cases, by using a penumbra width of 3.2 mm the PTV margin would be overestimated, the larger penumbra the smaller margin is needed.

In a different publication M. Herk have presented how to compute the values of Σ and σ [6]. For a group of patients daily imaging have been acquired for a number of fractions. From these images a position has error been measured, typically translation in in three directions. First the systematic and random error for each individual patient and direction is estimated as the mean and standard deviation of the errors respectively. The group systematic error M is the mean of all means and is expected to be small but often deviates from zero due to uncertainties in the treatment equipment (room lasers, couch and the iso-center of the machine). Σ is calculated as the standard deviation of the means. σ is the standard deviation of all individual standard deviations. However, when the number of fractions per patient are few the difference between the random errors is difficult to prove. In this case σ can be calculated as the root mean square of the individual random errors. M. Herk also states that as seen from the tumor there is no difference between the different type of errors (organ motion, setup and delineation). Therefore, these errors should be treated equally and added linearly. For the standard deviation of the errors this means that the errors should be added in quadrature.

When the number of fractions n is small, the random errors will not lead to a blurring of the dose. Each random error will cause a shift in the dose distribution with respect to the CTV for that fraction. By treating the random error as a part of the systematic error the effect of few fractions can be adjusted. Several authors (de Boer and Heijmen [34] and Gordon and Sieber [35]) have noted this limitation in the van Herk formula and suggest the following adjustment of Σ and σ.

$$\Sigma' = \sqrt{\Sigma^2 + \frac{\sigma^2}{n}} \tag{9}$$

$$\sigma' = \sqrt{\frac{n-1}{n}\sigma^2} \tag{10}$$

These adjusted values are then used in van Herks formula, equation (7) or (8). A consequence of having few fractions per patient is that the minimum dose on the CTV surface for a given patient is no longer constrained to lie in the same direction as the direction of the systematic error for that patient. In the formula above (8) it is assumed to do so. When Σ is large with respect to σ the direction of the minimum dose point on the surface of the CTV is determined mainly on the direction of the systematic error Σ. Therefore, when $\Sigma > \sigma$ the adjustment in equation (9) and (10) can be considered adequate for margin calculation according to equation (7) or (8). However, when $\Sigma < \sigma$ the position of the minimum dose to the CTV becomes increasingly widely spread over the CTV surface. The adjusted recipe above will overestimate the minimum dose to the CTV for any fixed margin. The minimum dose to the CTV always increases as the margin increases. This overestimation in minimum dose will result in setting margins that are lower than those required to meet the required clinical dose threshold. Further the calculated margin also depends on the penumbra width σ_p with respect to σ. If $\sigma_p << \sigma$ the dose distribution has a sharp gradient around the CTV the position of the minimum dose to the CTV to become spread over the CTV surface. However, if $\sigma_p >> \sigma$ the penumbra would be dominant in determining the delivered dose in all directions. In this case the minimum dose to the CTV would be well approximated by the dose in the direction of the systematic error and the adjusted version of van Herks formula (equation 9 ,10) would give an accurate estimation of the required margin [36].

2.5.1 Additional errors

Intra-fractional uncertainties such as respiratory movement can be taken into account by acquiring a 4D-CT or a slow scan CT in the reference CT[6]. A 4D-CT captures several images in different phases of the respiratory movement. In a slow scanning method, the CT scanner runs slowly, and multiple respiration phases are recorded per slice such that a mean position of the target is acquired. A disadvantage of slow CT scans is reduced resolution and that the exact position of the target in time is unknown. In both these methods the CTV can be extended to the internal treatment volume (ITV) such that the ITV encloses the the CTV in all positions throughout the movement.

Depending on the shape and size of the target, rotational errors and deformation may be significant.[26]

Accuray have reported the spatial resolution for their imaging devices in the Accuray Physics Essentials Guide [37]. For the kVCT imaging system ClearRT the spatial resolution in the transverse plane is that objects of diameter 1.0 mm, with center-to-center spacing of 2.0 mm, should be distinguishable. The longitudinal spatial resolution for Whole Body protocols, the nominal slice thickness at iso-center is 3.6 mm, and the FWHM of the Slice Sensitivity Profile is typically 4.2 mm. For the MVCT imaging system CTrue the spatial resolution in the transverse plane is that objects of diameter 1.6 mm, with center-to-center spacing of 3.2 mm, should be distinguishable in the image. The longitudinal spatial resolution for Whole Body protocols the FWHM of the Slice Sensitivity Profile is typically 7.2 mm $\pm$ 1.0 mm for a coarse pitch.

Several publications have been made on setup accuracy in radiotherapy and how sturdy immobilization and clear setup-protocols improve the accuracy. S.K. Hui et. al. have reported setup errors in Tomotherapy for different treatment regions using MVCT [38]. An aquaplast mask was used for head and neck immobilization and a VacLok vacuum bag was used for all other immobilization (chest, abdomen, legs, prostate, TMI). The positioning was made using room lasers and three-point localization tattoos. The reported 3D-average displacement vector v for global systematic errors for each treatment site as was; HN 5.11mm, chest 8.58mm, pelvis 9.05mm, prostate 7.51mm, legs 9.97mm, spine 9.03mm, TMI 15.73mm.

3 Material and Method

Two patient groups were enrolled in this study; 16 TMI patients (9 male and 7 female at a average age of 30 years ranging from 5-57 years) previously treated at the TomoTherapy (Accuray Inc., Madison, WI, USA) and positioned using 3-point localization and 4 TMI patients (three male and one female of average age 45 years ranging from 32 -57 years) treated at the Radixact (Accuray Inc., Madison, WI, USA) positioned using SGRT. Because of the limited timespan of this project and the fourth patient being treated late in the project process, section 3.3.2 and 3.3.3 only include the first three treated patients.

3.1 Clinical practice - TMI patient positioning

A whole-body phantom (Kyoto Kagaku, Kyoto, Japan), Figure 7, was used to imitate the TMI treatment process and to verify the OSS setup. The phantom was positioned according to the SUH TMI protocol in section 2.4.1. The phantoms arm did not fit in the field of view of the image. A reconstruction was therefore made to extend the FOV and include the arm. The images were then exported to the TPS Precision. Two structure sets were created. The body structure was created as an outline of the phantom surface and the CTV as all the phantoms skeletal tissue. A simple plan was then made only to enable opening the phantom as a patient at the machine. The body structure was exported to the OSS system to be used as the reference surface. The phantom was then brought to the Radixact and positioned on the couch. The optical surface system, Catalyst HD+, was used to position the phantom. The surface was optimized by changing time and gain on the three cameras. To avoid non-optimal surface matching due to the glossy and see-through surface of the phantom, matt beige nylon stocking was used. The stockings changed the surface of the phantom in some areas, mainly around the joints. This change was overlooked when the phantom was positioned. The surface color map was set to an acceptance of 4mm and the phantom was positioned according to the errors suggested by the system. Once the suggested iso-shift was less than $\pm$ 1 mm in all translational directions and the color map was green, a kVCT image was acquired and matched with the reference CT. The remaining suggested errors of the OSS and the errors from the verification image were compared. The result from the phantom measurement can be found in the Appendix (section 8.1).
To develop a positioning method for TMI patients a volunteer study was carried out, including an customized TMI immobilization and repeated repositioning sessions at the treatment couch. The immobilization was made according to the SUH TMI protocol but with the mask excluded. The goal was to find the smallest tolerance that could be used without being unreasonably time consuming. This was done both for the upper body and the legs.

3.1.1 Positioning Upper Body

The OSS color map tolerance was set to 4 mm and all cameras were optimized to obtain satisfactory surface coverage. The couch was moved according to the OSS calculated translations. To verify that the calculated deviation was reasonable the live and reference surface were visually compared, since swelling or weight-loss may affect the surface registration. If the calculated translation did not seem reasonable, the surfaces were matched manually by looking at rigid structures such as head, shoulders and pelvis. The color map was studied to find rotations or if the extremities needed to be adjusted. In figure 8 the upper body of the volunteer is positioned with 4 mm color map tolerance. The blue surface is the reference surface and the green the live surface. The calculated deviations are seen on the right in the image.

Figure 7: *Whole body phantom (Kyoto Kagaku, Kyoto, Japan) positioned in a TMI immobilization at the Radixact positioned with OSS system.*

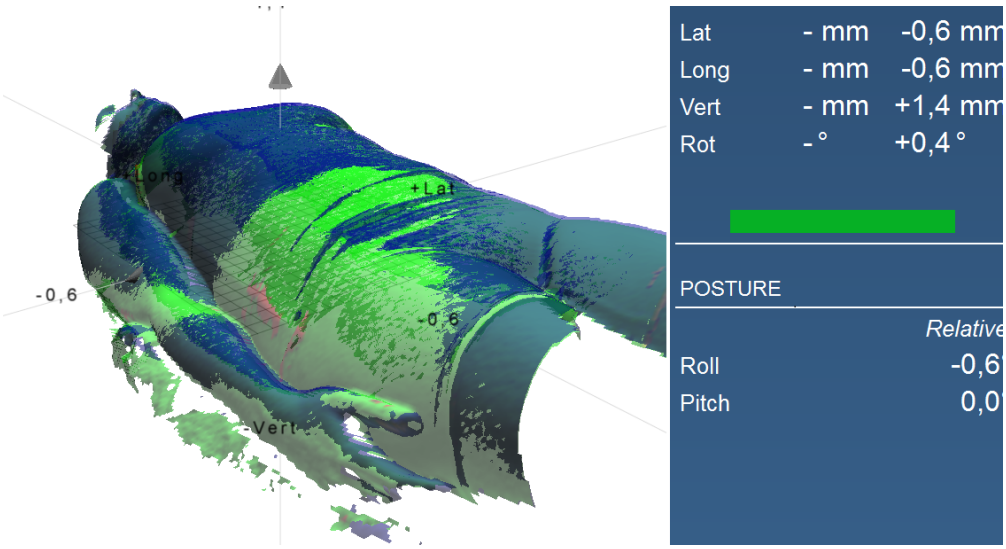

Figure 8: *Upper body of volunteer positioned using OSS system with color map tolerance 4 mm.*

3.1.2 Positioning Lower Body

The OSS color map tolerance was set to 5 mm and all cameras were optimized to obtain satisfactory surface coverage. The patient was not moved according to the calculated translations. Instead, the live and reference surface was compared to find necessary translations to move the couch. For translation in the longitudinal direction the knee and the bridge of the foot was studied. The color map was studied to find rotations or if the extremities needed to be adjusted. In Figure 9 the lower body of the volunteer is positioned with 5 mm tolerance. Figure 10 shows how the feet can be adjusted with help from the color map.

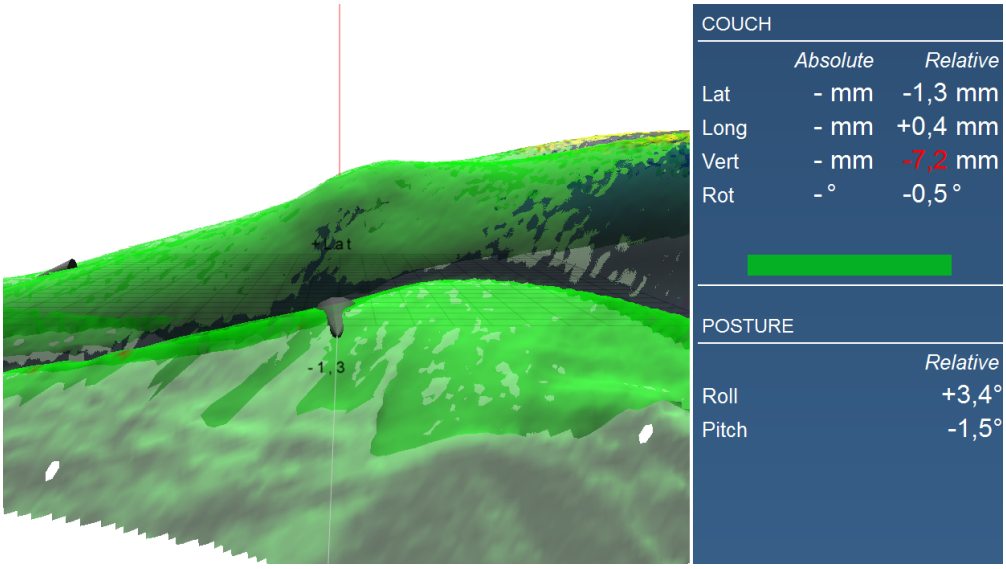

Figure 9: *Lower body of volunteer positioned using OSS system with color map tolerance 5 mm.*

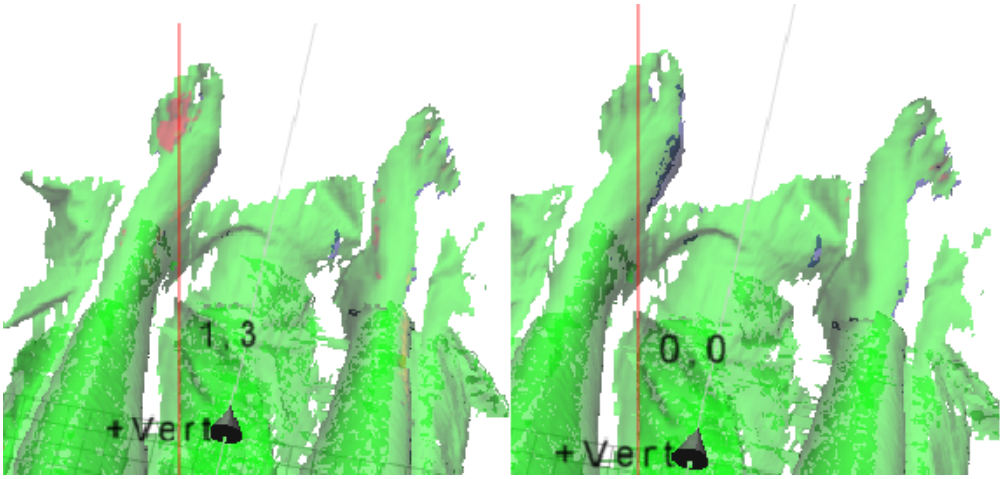

Figure 10: *The red area to the left indicates where the foot is misaligned to the planned position. This area is also seen on the foot, as a projected red light. The result after repositioning the foot is shown to the right.*

3.2 Retrospective three-point-localization setup

3.2.1 OSS system evaluation

Sixteen patients treated with TMI at the TomoTherapy with Catalyst as a assisting positioning tool were evaluated retrospectively. The patients had been positioned with three-point localization using lasers and tattoo markers with the OSS as an assisting tool to adjust mainly the extremities. The deviation from the MVCT verification image was compared with the suggested deviation from the OSS. The parameters vert, lat, long and roll were compared since these are the ones that can be corrected for without manually moving the patient. In some cases, the acquired surface was saved with a blanket covering the patient or once the patient had started translating through the bore. These data points were discarded.

3.2.2 Margin calculation

The errors obtained from the MVCT imaging were used to calculate systematic and random setup errors for the 16 patients. When studying the accepted image registration additional deviations were seen between the position of the CTV compared to the reference CT. The image registration was still accepted since the CTV was within the current PTV margin. However, the deviation for the accepted position did not represent the real error for the whole CTV. Since the CTV is large and not a rigid volume, no translation or rotation could give a perfect match over the whole CTV. Therefore the 6 sub-CTV's (skull, body without arms, arm(L/R) and leg(L/R)) were manually matched individually to find the remaining errors from the accepted registration. The six sub-CTV are displayed in Figure 11 where each CTV is delineated in pink with the current PTV margins in blue. The manual matching was performed in Precision - Review. From the clinically accepted registration, the "overall" error was found and in each sub-CTV, additional errors were found. For each patient and translation direction the systematic and random error were found according to the method described by M. Herk in section 2.5. Since the number of fractions for TMI is small (6 fractions) σ was calculated as the RMS of the random errors. This was done for the overall errors in the upper and lower body, as well as for each sub-CTV. The systematic and random error of the upper body was added in quadrature to the systematic and random error of each sub-CTVs that belonged to this image (skull, body without arms and arms(L/R)). The same thing was done for the lower body and each sub-CTV (leg L/R). From the calculated values of Σ and σ a margin for each sub-CTV was calculated. The margin was calculated both according to the van Herk formula, equation (8), and according to the adjusted van Herk formula, equation (9) and (10). Rotational errors were discarded. The discarded rotational errors would partly be accounted for when dividing the CTV into sub- groups. When matching a sub-CTV the rotation axis was in the middle of the whole CTV and larger rotations and translations would be required than if the rotation axis was centered in the sub-CTV. This was another reason for discarding the rotational errors. However, due to this limitation, additional errors in each sub-CTV were still found. Common regions for additional deviations for all the patients were recorded and used as additional sub-CTV in the following study.

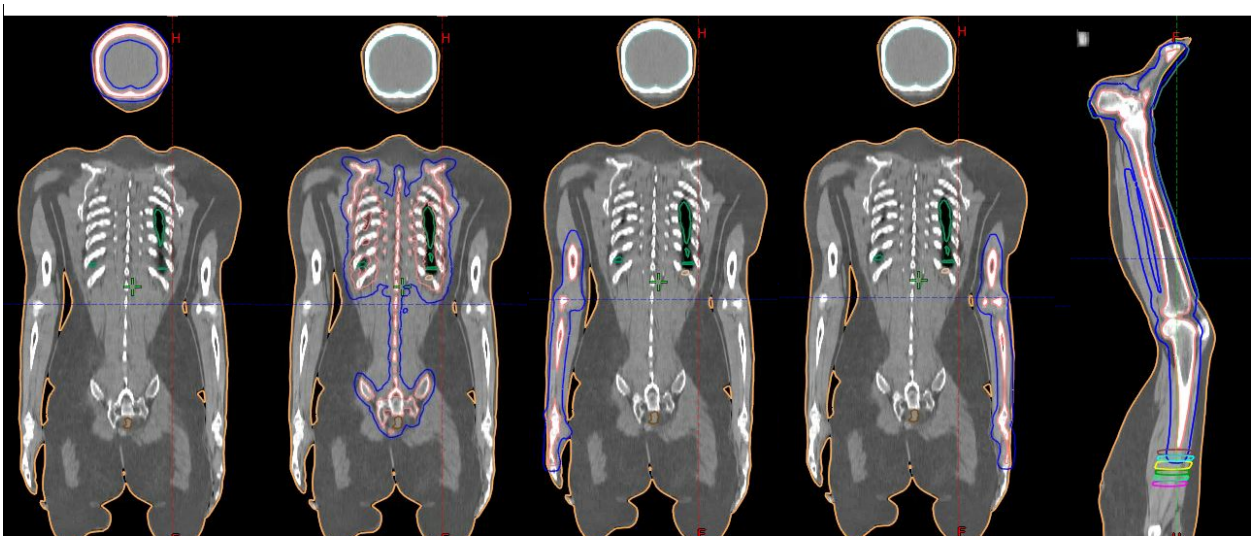

Figure 11: *Outlined sub-CTV (pink) and PTV (blue) structures. From the left: skull and neck, body without arms, arms (L/R) and legs (L/R).*

3.3 New surface guided setup

Within the frame of this study, four patients were treated with TMI using SGRT. The patients were positioned according to the method developed on the volunteer above, section 3.1.1 and 3.1.2. The patients were positioned using the OSS system and the posture was considered adequate when the live color map was green over the whole surface. In practice this was hard to achieve, some errors were seen but difficult to correct on the patient. Deviations from the green color was accepted if they were due to the patient's underwear, vascular access devices or other medical equipment. Deviations due to the patient respiration were also discarded. The OSS system's positioning ability was then evaluated with daily kVCT imaging as described in section 3.2.1. First the overall clinically accepted error was found before letting the patient proceed to treatment. The images were then analyzed again, in Precision Review, where each sub-CTV was matched manually. This time additional sub-CTV recorded in section 3.2.2 were included and matched. The sub-CTVs were skull, neck, thorax (body without arms and pelvis), pelvis (and femur until the junction), arms (L/R), hands (L/R), legs(L/R), feet (L/R). Although the CTV was further divided into sub-CTV additional deviations were seen both due to rotations and target deformations. Based on the measured errors, margins were calculated for each sub-CTV as done in section 3.2.2. Because of the limited timespan of this project the margin evaluation and verification is only including the first three treated patients.

3.3.1 Margin for cortical bone

To review the order of magnitude of the margin incorporated in the CTV the thickness of the cortical bone thickness was measured in four different locations for the three patients. The following sites were measured; temporal bone (supra-orbital plane), thoracic ribs (carina level), mid-line bone in pelvis, mid femur. All the sites were measured in the transverse plane. These bones were chosen since they all contain red bone marrow and represent different cortical bone thickness.

3.3.2 Margin evaluation

To evaluate how the calculated margins would affect TMI treatment the patients positioned using the SGRT-system were studied retrospectively. The new PTV margins for thorax (body without arms and pelvis) and pelvis (and femur until the junction) were applied on each patient. The treatment plans were then re-optimized using the new margins. The margins were created in Eclipse Contouring and the treatment plans were optimized in Accuray's Precision. The treatment plans were optimized to have the same PTV coverage as the original clinical treatment plan. The mean dose to 98% of the PTV was used to validate the same dose coverage in the two plans. When optimizing the dose with new margins, the same criteria to OARs as the original plan was used initially. The criteria to OARs were then gradually changed to reduce the dose up until the PTV coverage was no longer comparable to the original plan. The dose to OARs was then used to compare the two plans.

3.3.3 Margin verification

To verify if the new margins and the new treatment plan were sufficient to cover the target, the treatment plan was recalculated on the daily verification images. First the CTV structures were transferred from the reference CT to each verification kVCT. This was done using deformable image registration in Eclipse. However, the registration was not perfect, and the CTV had to manually be corrected in Eclipse Contouring. The images and CTV structures were then exported to the TPS and imported as phantoms for quality assurance (QA). The Hounsfield units (HU) were corrected according to the kVCT settings. The two images were

aligned by iso-center, the iso-center of the kVCT image (before matching and moving the couch) and the iso-center of the treatment plan. The new treatment plan was then calculated on the kVCT image. Since the dose gradient in the junction overlap the CTV, the CTV dose coverage was low in this region. Therefore, the volume of the CTV and junction overlap was calculated. This volume was then subtracted from the dos-volume-histogram and the new volume was treated as the 100% volume where the CTV coverage was evaluated. Although the margins were calculated to ensure that the minimum dose to the CTV is more than 95% of the prescribed dose, the minimum dose was not evaluated. This was to prevent the dose of one voxel determining the quality of the plan. Instead the dose covering 99.5% of the volume ($D_{99.5\%CTV}$) was used to evaluate the six fractions of the three plans. The kVCT images were also analyzed for the original plan. The dose coverage of the new and original plans was compared using a paired Wilcoxon test.

Finally, a fourth patient was treated with TMI. The patient was positioned with the same method as the other three patients and daily images were acquired. The sub-CTVs were matched, and the margins were recalculated.

4 Result

4.1 OSS system evaluation

The difference between the OSS system's calculated deviation and the deviation from the matched verification image is presented as a box plot (Figure 12). Crosses mark the mean value, lines the median value, boxes the exclusive first and third quartile and the whiskers the maximum and minimum value (outliers excluded). The figures present the deviation in 4 degrees of freedom (lat, long, vert and roll) and the results from the 16 patients positioned using 3-point localization at the TomoTherapy and the 4 patients positioned using the SGRT-system at the Radixact are presented separately. The mean and the standard deviation for the two patient groups and the four deviation parameters are also presented in Table 1.

Table 1: *Mean and standard deviation of the difference between the OSS system's and the verification image's calculated deviation for the patients positioned using 3-point localization and the patients positioned using the SGRT-system for the lower and upper body.*

	ΔLat [mm]		ΔLong [mm]		Δ Vert [mm]		Δ Roll [deg]	
Upper body	SGRT	3-pt loc	SGRT	3-pt loc	SGRT	3-pt loc	SGRT	3-pt loc
Mean	-0.09	-0.97	-2.6	-0.28	-2.8	-1.5	-0.01	-0.38
SD	1.3	1.5	1.7	3.0	2.6	5.6	0.46	0.98
Lower body	SGRT	3-pt loc	SGRT	3-pt loc	SGRT	3-pt loc	SGRT	3-pt loc
Mean	-0.13	0.08	-1.8	-2.2	-1.2	-1.4	0.29	-0.27
SD	2.0	3.0	2.6	5.0	3.6	10.1	2.4	3.3

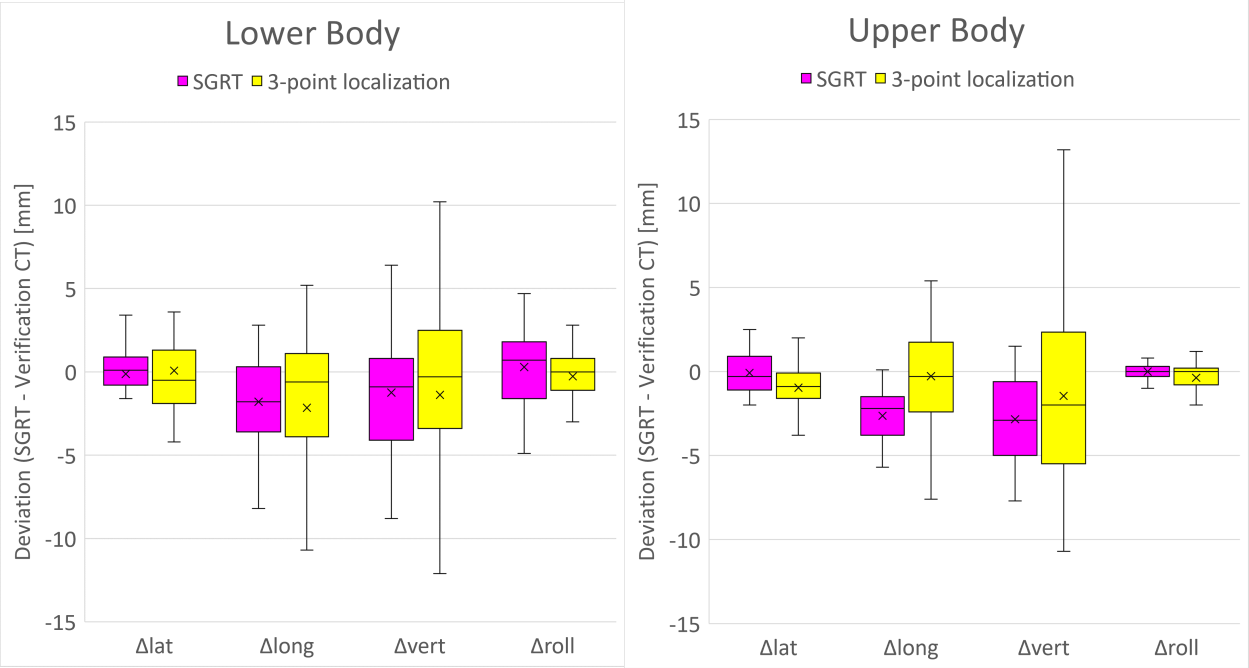

Figure 12: *Difference between the OSS system's and the verification image's calculated deviation for the patients positioned using 3-point localization and the patients positioned using the SGRT-system for the lower and upper body. Crosses mark the mean value, lines the median value, boxes the exclusive first and third quartile and the whiskers the maximum and minimum value (outliers excluded).*

4.2 Overall error

The clinically accepted "overall" error for the 16 patients positioned using 3-point localization and the 4 patients positioned using the SGRT-system are presented in Table 2 and 3. The errors are presented as systematic Σ and random calculated as the standard deviation of all patients individual standard deviation σ and as the root-mean-square of the individual standard deviation $\sigma(RMS)$. To compare the two groups a margin is also presented, calculated according to equation (8) with α=2.5 and γ= 0.7 and $\sigma' = \sigma(RMS)$.

Table 2: *The overall error of the upper body presented as systematic Σ, random as σ and $\sigma(RMS)$ and a margin calculated according to equation (8) for the patients positioned using 3-point localization and the patients positioned using the SGRT-system.*

Thorax	Lat [mm]		Long [mm]		Vert [mm]	
	SGRT	3-pt loc	SGRT	3-pt loc	SGRT	3-pt loc
Σ	0.54	1.17	0.14	1.86	1.89	1.63
σ	0.25	0.86	0.32	0.73	0.62	1.44
$\sigma(RMS)$	1.18	1.43	1.1	1.84	1.25	2,96
Margin	2.19	3.93	1.11	5.92	5.6	6.14

4.3 Margin - three-point localization

The calculated margins for the patients positioned using 3-point localization are presented in each translation direction and for each sub-CTV in Tabel 4. The margins are calculated according to the van Herk formula,

Table 3: *The overall error of the lower body presented as systematic Σ, random as σ and $\sigma(RMS)$ and a margin calculated according to equation (8) for the patients positioned using 3-point localization and the patients positioned using the SGRT-system.*

Legs	Lat [mm]		Long [mm]		Vert [mm]	
	SGRT	3-pt loc	SGRT	3-pt loc	SGRT	3-pt loc
Σ	0.53	1.56	0.21	1.61	0.43	1.51
σ	0.7	0.93	0.45	0.73	0.48	0.91
$\sigma(RMS)$	1.23	1.47	1.9	1.33	1.38	1.5
Margin	2.19	4.93	1.86	4.95	2.04	4.84

equation (8), and with the adjusted Van Herk formula, equation (8), (9) and (10).

Table 4: *Margins for each sub-CTV and direction calculated with the van Herk formula and the van Herk formula adjusted for 6 treatment fractions for the patients positioned using 3-point localization.*

Van Herk Formula			
	Lat [mm]	Long [mm]	Vert [mm]
Skull	4.6	8.7	7.3
Body	4.6	7.6	7.3
Arm R	5.3	9.6	7.9
Arm L	5.2	8.4	8.2
Leg R	6.8	6.3	5.7
Leg L	5.8	7.2	5.6

Adjusted Van Herk Formula			
	Lat [mm]	Long [mm]	Vert [mm]
Skull	5.2	9.0	8.3
Body	5.1	8.2	8.5
Arm R	5.7	10	8.9
Arm L	5.7	9.2	9.3
Leg R	7.1	6.6	6.1
Leg L	6.1	7.4	6.0

When manually matching the six sub-CTVs the following structures were recorded to repeatedly have additional errors. CTV-skull; deviations in cervical spine, CTV-body; deviations in pelvis and sacrum, CTV-arms; deviations in hands, CTV-legs; deviations in feet.

4.4 Cortical Bone Thickness

The cortical bone thickness was measured to on average be; temporal bone 4.3 mm, thoracic ribs 3.2 mm, mid-line bone in pelvis 3.7 mm, femur 11 mm for the patients positioned using the SGRT-system.

4.5 Margin - SGRT

The calculated margins for the patients positioned using the SGRT-system are presented in each translation direction and for each sub-CTV in Tabel 5. The margins are calculated according to the adjusted Van Herk formula, equation (8), (9) and (10). Suggested clinical margins are also presented in Table 5.

Table 5: *Margins with additional sub-CTVs for SGRT positioning calculated according to the adjusted van Herk formula along with a clinical margin suggestion.*

Adjusted Van Herk Formula			
	Lat [mm]	Long [mm]	Vert [mm]
Skull	4.8	4.2	7.3
Neck	6	4.1	9.6
Thorax	4.4	4.2	7.1
Pelvis	7.7	3.5	7.6
Arm R	7.9	10.4	7.3
Arm L	5.7	6.6	7
Hand R	7.0	9.0	8.4
Hand L	6.8	4.8	8.1
Leg R	4.8	5.0	4.9
Leg L	4.4	5.9	4.1
Foot R	4.7	5.5	5.5
Foot L	5	5.5	6.8

Suggested Margins			
	Lat [mm]	Long [mm]	Vert [mm]
Skull	5	5	7
Neck	6	5	10
Thorax	5	5	7
Pelvis	8	4	8
Arm (L/R)	10	10	10
Hand (L/R)	10	10	10
Leg (L/R)	6	6	6
Foot (L/R)	6	6	6

4.6 Margin evaluation - Dose reduction to OAR

The mean dose to OARs are presented in Table 6 as the average over each patient group, along with the dose to 98% of the PTV $D_{98\%PTV}$. 3-pt represent the 16 patients positioned using 3-point localization with a PTV(body) margin between 8-10 mm depending on patient size. SGRT 8 mm represent the original clinical plan of the patients positioned using the SGRT-system. SGRT new margin represents the same patients, but the recalculated treatment plan based on the new suggested margins. All doses are weighted for a prescribed dose of 12 Gy although this might not have been the clinically delivered dose. As a reference, the dose to OARs for conventional TBI performed with lung shielding are presented in Table 6 based on a study by Svahn-Tapper G. et. al [39]. For OARs that are not shielded the dose depend on the location of the organ with respect to the depth-dose curve of the treatment. The dose for these OARs is presented as the prescribed dose but may be higher or lower than the prescribed dose. The mean OAR dose for the different treatment techniques is also visualized in a plot (Figure 13).

Table 6: *Comparison of mean dose to OARs for TBI treatment, TMI with a PTV(body) margin between 8-10 mm, TMI for the original treatment plan (PTV(body) 8 mm) and for the treatment plan with the new margins.*

	$D_{98\%PTV}$	Bowel Bag	Heart	Kidney L	Kidney R	Liver	Lung L	Lung R	Genitalia
TBI [Gy]		12	12	12	12	12	9.6	12	12
3-pt 10-8mm [Gy]	11.4	6.6	7.17	7.61	5.76	7.21	8.83	8.42	8.66
SGRT 8mm [Gy]	11.24	6.31	7.11	5.29	5.31	7.48	8.86	8.35	9.28
SGRT new margin [Gy]	11.22	5.67	6.69	4.66	4.88	6.96	8.61	8.19	8.97

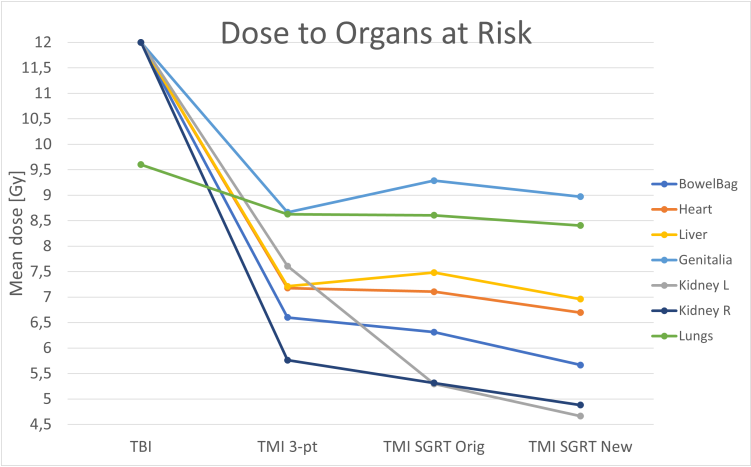

Figure 13: *Mean dose for different OARs and the different treatment techniques.*

A comparison between the original clinical plan and the re-calculated plan with new margins based on the novel surface guided setup method is presented for selected OARs below.

Bladder

The mean dose to the bladder was reduced between 5-8% with the new margins. This was an average reduction of 0.53 (range 0.42 - 0.72) Gy. The minimum dose was on average reduced from 5.1 Gy to 4.5 Gy. The maximum dose was on average increased from 11.8 Gy to 12 Gy.

Bowel bag

The mean dose to the bowel bag was reduced by 6-16% with the new margins. This was an average reduction of 0.64 (range 0.34 - 0.91) Gy. The minimum dose was on average reduced from 2.5 Gy to 2.1 Gy. The maximum dose was on average increased from 12.1 Gy to 12.5 Gy.

Genitalia

The mean dose to the genitalia was reduced by 4 - 9% with the new margins, an average reduction of 0.31 (range 0-0.68) Gy. For one patient the mean dose to genitalia was increased by 1% (0.12 Gy). The minimum dose was on average reduced from 3.8 Gy to 3.7 Gy. The maximum dose was on average increased from 12.1 Gy to 12.4 Gy.

Heart

The mean dose to the heart was reduced by 1-12% with the new margins, on average a reduction of 0.42 (range 0.06 - 0.79) Gy. The minimum dose was on average reduced from 3.2 Gy to 2.7 Gy. The maximum dose was on average reduced from 12.1 Gy to 11.9 Gy.

Liver

The mean dose to the liver was reduced by 4-11% with the new margins, on average reduced by 0.52(range 0.28-0.83) Gy . The minimum dose was on average reduced from 2.8 Gy to 2.6 Gy. The maximum dose was on average increased from 12.3 Gy to 12.4 Gy.

Kidney

The mean dose to the kidneys was on average reduced by 0.53 (range 0.24-1.18) Gy with the new margins, a reduction between 6-24% . The minimum dose was on average reduced from 2.9 Gy to 2.5 Gy. The maximum dose was on average reduced from 11.5 Gy to 11.1 Gy

Lungs

The mean dose to the lungs was reduced by 1-4% with the new margins, an average reduction of 0.21 (range 0.05-0.34)Gy. The minimum dose for the total lung volume was on average reduced from 2.7 Gy to 2.6 Gy. The maximum dose for the total lung volume was on average increased from 12.4 Gy to 12.5 Gy. The total lung volume receiving 5 Gy or more V_{5Gy}, was for one patient unchanged for the new treatment plan and for the other two patients reduced by 1.3 and 2.2 % respectively.

Rectum

The mean dose to rectum was on average reduced by 0.77 (range 0.59-0.94) Gy with the new margins, a reduction of 8-9%. The minimum dose was on average reduced from 5.9 Gy to 5.1 Gy. The maximum dose was on average increased from 11.9 Gy to 12 Gy.

Target coverage

The target coverage, in terms of the dose covering 98% of the PTV $D_{98\%PTV}$, of the original plan compared to the new plan differed 0.1 Gy, 0.08 Gy and 0.06 Gy for the three patients respectively.

4.7 Margin verification - Target coverage

In figure 14 the dose to 99.5% of the CTV, $D_{99.5\%CTV}$ is presented as the cumulative dose over the delivered fractions for each patient. The plots show $D_{99.5\%CTV}$ for the original plan and the new plan with the new margins along with the prescribed dose (2 Gy/fraction). The total delivered $D_{99.5\%CTV}$ for the new and original plan was 94,67% and 95,92%, , 95,67% and 96,58%, 93,63% and 91,67% for the three patients respectively. The average fraction dose for $D_{99.5\%CTV}$ was 1.92 (1.81 – 1.94) Gy and 1.92 (1.71 – 1.94) Gy for the original plans and the new plans, respectively. There was no significant difference ($p<0.05$) observed.

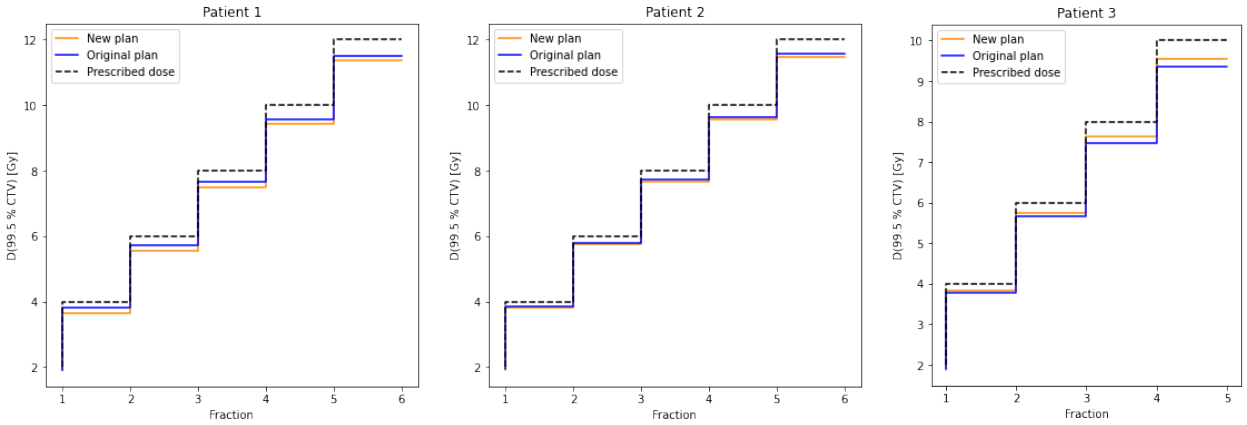

Figure 14: *$D_{99.5\%CTV}$ cumulative dose as a function of the treatment fractions for each patient respectively. $D_{99.5\%CTV}$ of the original and new plan presented along with the prescribed dose.*

5 Discussion

5.1 OSS verification

As seen in Figure 12 the deviation between the OSS system and the verification image seems to be smaller for the patients positioned using the SGRT system than the 3-point localization. The large deviation in the vert direction for the patients positioned using 3-point localization can be explained by the couch sag at the TomoTherapy where these patients were treated. Since the couch sag depend on the weight of the patient it is more evident for the upper body. Although the couch sag is a known default at the TomoTherapy it was not correct for it when studying the deviations. This was because the reference surface was corrected vertically with an estimated couch sag either before the first fraction or after the verification image of the first fraction. This means that the deviation from the couch sag is greater for the first fraction but depend on the patient and how it had been corrected for. The other parameters also appear to deviate less for the patients positioned using the SGRT system than the 3-point localization. One reason for this could be the poor resolution of the MVCT causing larger uncertainties in the verification image for the patients treated at TomoTherapy than the Radixact. Another reason could be that the patients treated at the TomoTherapy were not corrected according to the calculated deviations of the OSS. For the SGRT group, after moving the couch according to the OSS suggestions, the surfaces are registered again, and an additional correction may be performed. Since the registration is a iterative process the new position will give a better initial guess of the position and the calculation will reach a better result. This also applies to the lower body where the surfaces are visually matched, and the initial guess will be closer to the accurate position.

To possibly further improve the OSS system's positioning ability, a different surface registration method could be evaluated. Instead of letting the registration being weighted higher close to the iso-center it can be weighted for points close to the PTV. This could be a topic for further research. The new Catalyst HD+ system also enables motion management during HT by tracking the couch. This is installed at the TomoTherapy and Radixact but is not yet clinically in use. By tracking the patient during treatment one can assure that the patient does not move. This could further justify decreasing margins. One issue with motion management is that the patient cannot wear a blanket in the cold treatment room and is especially an issue for TMI with treatment times up to 20 minutes.

5.2 Margin calculation

Table 2 and 3 suggests that the overall positioning errors have been reduced when positioning with SGRT at the Radixact in comparison with the 3-point localization at the TomoTherapy. Both the systematic and the random errors for all directions are reduced apart from the vertical systematic error of the upper body and the longitudinal random error of the lower body. However, when combining the random and systematic error into a margin the reduction applies to all directions. This indicates that a better positioning is achieved with OSS as the main positioning tool. To decide whether this reduction is significant a larger patient group is needed.

As seen in Table 4 the margins are larger when calculated with the adjusted van Herk formula. Since TMI is treated with six fractions which is not enough for the random errors to cause a blurring of the dose, the adjusted van Herk formula was chosen. The calculations are made with the assumption of a penumbra width = 3.2 mm. As stated in section 2.5 authors have suggested larger penumbra width for VMAT treatments. HT treatments are intensity modulated similar to VMAT and the penumbra width was therefore

assumed to not be smaller than 3.2 mm. Based on this the calculated margins should not have been underestimated. Since the overall random error for all directions is smaller than the chosen penumbra width of 3.2 mm the adjusted van Herk formula should give an accurate estimation of the required margin. The adjusted van Herk Formula in Table 4 indicates that the margins can be reduced for some sub-CTVs for patients treated at the TomoTherapy. The measured deviations in each sub-CTV were matched manually by visually studying the verification and reference image. The uncertainty of the manual registration is greater in the longitudinal direction since the resolution is larger in this direction. Generally, the uncertainty would also be larger for the TomoTherapy than the Radixact since the kVCT have a better resolution. The poor resolution of the MVCT also made it difficult to estimate how large the recorded additional deviations of the neck, pelvis, hands and feet were. Therefore, these structures were divided into sub-CTVs when studying the patients treated at the Radixact.

The margins in Table 5 are based on 18 fractions of the three patients treated at the Radixact. The new positioning method seem to not only improve the overall error but also the error of each sub-CTV. The calculated margins are the smallest safe margin and therefore in the suggested clinical margins the numbers were rounded up to the nearest integer. The difference between hands and arms and feet and legs were small, and therefore not divided into sub-CTVs. Since there are no OARs adjacent to arms and legs it was also not clinically justified in comparison to the extra work required. For the skull and neck as well as the body and pelvis the difference were larger and the potential sparing of OARs more significant. As seen in Table 5 the margins for skull, neck, body and pelvis were suggested to be reduced compared to the current margin protocol (7 mm and 8 mm respectively). The only region where the current margins were insufficient was in the vertical direction of the neck. This is in agreement with the recorded deviations seen when matching patients treated at the TomoTherapy. Positioning of the neck seems to be a reoccurring challenge for both groups. The margin of the legs can be reduced from 10 to 6 mm. The measured deviations of each sub-CTV contain uncertainties depending on the resolution of the kVCT image. The largest uncertainties is in the long direction where the resolution is 4.2 mm. Since the sub-CTVs overlap each other and the junction has a dose fall off in the long direction this should not have a great impact on the margin. The resolution in the transverse plane is 1.6 mm and affect the uncertainty in the lat and vert direction. For the 3 patients the additional margin incorporated in the CTV, the thickness of the cortical bone, ranged between 3.2- 11 mm. The uncertainty of the delineation of the CTV can be neglected since bone tissue is distinguishable from surrounding tissue in comparison to other tumor tissues, and is in majority delineated automatically with segmentation by HU values. Although the sub-CTVs were further divided for this patient group additional errors were still seen. These errors were due to rotation or deformation such as finger separation and spine arch. Since the review image registration software could not move the rotational axis to the concerning sub-CTV it was difficult to measure the magnitude of the additional deviations. Instead, the new suggested margins were evaluated on the daily kVCT images to verify if they are sufficient. To reduce the uncertainties of the manual registration the errors in each sub-CTV could have been found with an automatic registration on bone tissue. The overall error was found by automatically registering the bones in the two images. For Precision's image registration, this technique is only available for the whole image. If it would have been possible to apply a ROI, each sub-CTV could have been matched automatically and eliminating the bias of the user.

These margins are calculated to ensure adequate dose without daily imaging. A verification image the first two or three fractions to ensure that there are no gross errors should be enough. For a TMI protocol with daily imaging the margins can be reduced further. In case of daily imaging, the overall error can be

removed from the margin calculation and only depend on the errors of each sub-CTV.

5.3 Margin Evaluation - Dose reduction to OAR

Using the new margins, the average of the mean dose to all OARs was reduced. According to the theory this can potentially reduce the incidents of both acute and late side effects. How much the dose could be reduced depended on the optimization of the original plan and the patient's individual anatomy. The reduced dose to genitalia was restricted for 3 of the patients where the testis was included in the CTV. The difference between TMI and TBI mean dose to the lungs is only approximately 1 Gy. However, for TBI the whole lung receives approximately 9.6 Gy. This means that the minimum dose for the lung is 9.6 Gy and V_{5Gy} is 100%. With TMI V_{5Gy} is reduced to approximately 75% and further reduced with the new margins. This reduces the risk of pneumonitis. This is why the mean as well as the maximum and minimum dose is presented. For most OARs the new plan had a slight increase in maximum dose. For many OARs the PTV overlap the organ and cause a high maximum dose in this region. For parallel organs such as heart, lungs, liver, kidney and bladder the mean dose is more important to minimize in order to reduce side effects. For serial organs such as the bowel bag, minimizing the maximum dose of more clinical value. From this perspective, for the bowel bag the new treatment plans are not favorable since they did not archive a lower maximum dose. However, note that the maximum and minimum dose can be determined by the dose of one voxel. To determine the biological hazard on the OARs further dose-volumes should be studied. Although the dose reduction to the OARs may seem small, for these heavily treated patients any dose reduction would be beneficial. Since the whole patient is irradiated a reduced minimum dose to several OARs, results in a reduced integral dose. Although the integral dose is not used when evaluating the plan, the integral dose can be of importance and should be kept at a minimum as long as the tumor dose is not compromised.

To conclude that the reduced margins result in a significantly reduced dose to OARs more patients need to be included in the study. To draw any conclusion of what effect these margins would have, a follow-up study could be performed where patients are treated with reduced margins and the side effect and relapse-rate could be studied. Since all dose to OARs is an unnecessary hazard, the reduced margins for these patients would be beneficial.

For future studies the margins for skull and neck could be evaluated and the dose to oral cavity and eye lenses studied. Although there are no OARs close by the legs this study suggests an isotropic reduction of the margins for the legs by 4 mm. Presumably, this margin reduction is of small clinical importance, however, as a principle all unnecessary dose should be avoided.

5.4 Margin verification - Target coverage

No significant difference in $D_{99.5\%CTV}$ between the new and the original plans were seen. The dose coverage of the two plans are comparable. For patient 1 and 2 $D_{99.5\%CTV}$ was slightly higher for the original plan than the new plan, $D_{99.5\%CTV}$ was approximately 95% which is considered satisfactory. Since the treatment plan is made in order for the 95% isodose surface to cover most of the CTV, a 95% dose to 99.5% of the CTV is reasonable. For patient 3 the $D_{99.5\%CTV}$ was lower and the new plan had better coverage than the original plan. This seemed concerning and the treatment plans and kVCT images were further studied. The 95 % and 93% isodose curves covered most parts of the CTV, and the low dose coverage was originating from the region of the junction. The original plan had a region of under dosage right before the start of the junction. This had been compensated for in the plan for the lower body in the dose overlap. Only evaluating

the upper body was not a fair representation of the dose coverage in the junction. This was probably the reason why $D_{99.5\%CTV}$ was higher for the new plan. Another reason why both plans for patient 3 had a low $D_{99.5\%CTV}$ was also found in the junction. A disposition was found in the long direction although the junction lead markers were perfectly matched in the kVCT image and the treatment plan. The shift was seen from the femoral head and pelvis when comparing the dose distribution in the reference CT and the kVCT. By measuring the distance from the femoral head and the lead marker in the reference and kVCT a difference of 0.7-1 cm was found. This made the dose distribution shift in long direction and made a larger part of the femur included in the junction. The incorrectly placed lead marker could either be due to the skin of the legs moving or the lead markers being placed in the wrong place. To prevent this the junction could be marked internally, as a distance from the femoral head, instead of outside the body. The actual effect of this on patient 3 would not be as large. Firstly, the patient was corrected a few mm in the long direction before treatment and secondly, the junction markers were in the same location for the lower body and the dose fall-off would compensate for the under dosage in the upper body -plan.

To reduce the margins further, the actual target volume, the bone marrow, could be evaluated instead of all bone tissue. By doing this the cortical bone would not be included in the CTV but be a part of the PTV. However, doing this would increase the workload since the bone marrow cannot be delineated automatically. If the cortical bone is excluded from the CTV other uncertainties, such as image resolution, delineation error and uncertainties in the machine isocenter, should not be neglected in the margin calculation.

6 Critical reflection

It should be noted that the observed difference between the two patient groups does not just reflect the difference of two positioning methods but also different treatment machines. The TomoTherapy have three major factors that may affect the errors presented in this rapport. Firstly, the poor resolution of the MVCT images acquired at the TomoTherapy will cause a larger uncertainty in the measured position errors in comparison to the kVCT images at the Radixact. Secondly, the couch sag at the TomoTherapy will cause a larger positioning error in the vertical direction. Finally, the whole-body MVCT images take a lot longer to acquire than the kVCT images (approximately 20 minutes and 1.5 minutes respectively). The longer on couch-time increases the risk of patient movement. Therefore, at the TomoTherapy, this is a greater source of error.

Black sheets were placed between the patient and the white immobilization, this was to detect as little reflections from the immobilization as possible. In some cases, the mask and other medical equipment disturbed the live surface. However, since the registration is deformable it should not affect the calculated displacement. In some cases, it did make it harder to visually match the surfaces.

When positioning the lower body with the OSS system, the suggested couch displacement was discarded. When moving according to the suggestion, large deviations were visually seen between the two surfaces. The incorrect surface registration is presumably due to the registration being weighted towards points near the iso-center and the iso-center in the lower body being located in between the legs. This is why the lower body was matched visually. To visually see how much and in what direction to correct the couch but also the individual limbs is not trivial and require practice. For both the upper and the lower body, the hardest direction to visually match was the longitudinal. When studying the color map, difficulties were encountered

when distinguishing rotational errors from latitudinal displacements. For the upper body the calculated registration was more accurate. For one patient, due to swelling over the abdomen, vertical deviations were seen over the shoulders and head in the two surfaces after correcting according to the calculated registration. The iso-center for the upper body is in mid-thorax. Therefore, in the registration, the abdomen was weighted higher than the head. This is why, in the method description, the upper body can be position according to the calculated registration but should also be controlled visually on more rigid structures such as shoulders and pelvis. Since the lower body is only matched visually the surface registration should perhaps be improved, before implementing SGRT for the lower body fully. This to prevent the positioning being biased by the radiotherapy staff and have consistent positioning for all TMI patients.

Other difficulties seen in regard to the OSS system was artefacts in the reference surface when an extended FOV was used for the reference CT. This made is hard to visually match the surfaces. To solve this, for larger patients where extended FOV is necessary, a reference surface could be captured with the OSS when acquiring the reference CT instead of using the outlined body structure. The patients wore close-fitted net-underwear during treatment to disturb the surface as little as possible. For one patient with dark skin the white underwear got overexposed when the OSS cameras were optimized to visualize the surface of the patient. This made the patient's pelvic area undetected in the live surface. This is solved by using darker underwear when necessary. At times deviations were seen in the OSS system but could not be corrected for physically. The deviations could either be due weight loss, swelling of the patient or due to the immobilization vacuum bag changing shape as the patient climb onto the couch. This was mainly a challenge when adjusting the arms and hands. To prevent this an alternative immobilization of the arms and hands could be considered.

When the errors of patient number 4 were included in the calculated margins the margins changed. These margins are not presented in the report but should be included in future studies. One of the patients in the presented margin calculation showed large deviations in the vertical direction due to swelling. The deviation of this patients gave less impact when the fourth patient was included in the calculation and the margin in the vertical direction was reduced. This is to expect and shows that a larger population is needed when calculating these population-based margins. To find the appropriate margin for HT-TMI as a patient group more patients need to be included in the derivation.

When evaluating the new margins only the treatment plan for the upper body was remade and only the margin for the thorax and pelvis was adjusted. Most OARs are adjacent to these sub-CTVs and were therefore considered most valuable to evaluate. When comparing the original and new plans the dose coverage of 98% of the PTV were unchanged. Since the dose fall-off is a part of the PTV, the coverage is lower than the criteria that the 93% isodose curve should cover the whole PTV. Since the volume of the dose fall-off is the same in both plans but the PTV is smaller in the new plan the impact of the dose fall-off is larger in the new plan. This means that although the dose of 98% of the PTV was unchanged the dose coverage of the PTV outside the junction is higher for the new plan. To avoid this the volume of the PTV with the junction excluded could have been evaluated for the two plans. It should also be noted that it is difficult to compare different treatment plans since they are performed with different dose constraints, different number of iterations and by different users. For a more fair comparison both plans should be created by the same user.

When evaluating the treatment plan on the verification images the CTV was transferred from the reference CT to each kVCT image. The CTV overlaps parts of the junction and this volume is not irradiated

with 100% of the dose. When evaluating the CTV dose coverage in the kVCT images this made the minimum dose low. Therefore, the volume of the CTV-junction overlap was subtracted from the dose-volume histogram. The subtracted volume did not necessarily correspond to the overlap but could be other underdosed regions of the CTV. Therefore the dose coverage $D_{99.5\%CTV}$ might not be an accurate representation of the delivered dose. To evaluate the dose coverage accurately the overlap volume should be removed from the CTV structure in the kVCT images. However, the method should be sufficient to compare the new and the original plan.

7 Conclusion

Based on this study, Surface Guided Helical Tomotherapy for Total Marrow Irradiation suggests to improve patient positioning. Compared to current margins, the improved positioning can warrant reducing margins for the skull, thorax, pelvis and legs. With reduced margins for the thorax and pelvis, the mean dose to the bladder, heart, lungs, kidneys, bowel bag, liver, rectum and genitalia can be reduced while maintaining satisfactory target coverage.

References

[1] Cancerfonden. 2021. Leukemi – Symtom, orsaker och behandling. [online] Available at: <https://www.cancerfonden.se/om-cancer/cancersjukdomar/leukemi?gclid=EAIaIQobChMInIqkzcah 8wIVhdKyCh2ZXwboEAAYASAAEgLyL$_{DB}$wE > [$Accessed 16 December$2021].

[2] Wong, J., Filippi, A., Dabaja, B., Yahalom, J. and Specht, L., 2018. Total Body Irradiation: Guidelines from the International Lymphoma Radiation Oncology Group (ILROG). International Journal of Radiation Oncology*Biology*Physics, 101(3), pp.521-529.

[3] Hoeben BAW, Pazos M, Albert MH, Seravalli E, Bosman ME, Losert C, et al. Towards homogenization of total body irradiation practices in pediatric patients across SIOPE affiliated centers. A survey by the SIOPE radiation oncology working group. Radiotherapy and oncology : journal of the European Society for Therapeutic Radiology and Oncology. 2021;155:113-9.

[4] Rassiah P, Esiashvili N, Olch AJ, Hua CH, Ulin K, Molineu A, et al. Practice Patterns of Pediatric Total Body Irradiation Techniques: A Children's Oncology Group Survey. Int J Radiat Oncol Biol Phys. 2021.

[5] Änghede Haraldsson, A., 2021. Helical tomotherapy for total marrow and total skin irradiation : Optimisation, verification, and clinical results.

[6] van Herk, M., 2004. Errors and margins in radiotherapy. Seminars in Radiation Oncology, 14(1), pp.52-64.

[7] ucsfbenioffchildrens.org. 2022. Conditioning Regimen for a BMT. [online] Available at: <https://www.ucsfbenioffchildrens.org/education/conditioning-regimen-for-a-bone-marrow -transplant-bmt> [Accessed 7 January 2022].

[8] Buchali A, Feyer P, Groll J, Massenkeil G, Arnold R, Budach V. Immediate toxicity during fractionated total body irradiation as conditioning for bone marrow transplantation. Radiotherapy and oncology : journal of the European Society for Therapeutic Radiology and Oncology. 2000;54:157-62.

[9] Haraldsson, A., Wichert, S., Engström, P., Lenhoff, S., Turkiewicz, D., Warsi, S., Engelholm, S., Bäck, S. and Engellau, J., 2021. Organ sparing total marrow irradiation compared to total body irradiation prior to allogeneic stem cell transplantation. European Journal of Haematology, 107(4), pp.393-407.

[10] Leung W, Hudson MM, Strickland DK, Phipps S, Srivastava DK, Ribeiro RC, et al. Late effects of treatment in survivors of childhood acute myeloid leukemia. J Clin Oncol. 2000;18:3273-9.

[11] Kunkele A, Engelhard M, Hauffa BP, Mellies U, Muntjes C, Huer C, et al. Long-term follow-up of pediatric patients receiving total body irradiation before hematopoietic stem cell transplantation and post-transplant survival of >2 years. Pediatric blood cancer. 2013;60:1792-7.

[12] Mulcahy Levy JM, Tello T, Giller R, Wilkening G, Quinones R, Keating AK, et al. Late effects of total body irradiation and hematopoietic stem cell transplant in children under 3 years of age. Pediatric blood cancer. 2013;60:700-4.

[13] Willard VW, Leung W, Huang Q, Zhang H, Phipps S. Cognitive outcome after pediatric stem-cell transplantation: impact of age and total-body irradiation. J Clin Oncol. 2014;32:3982-8.

[14] Haraldsson, A., Ceberg, S., Ceberg, C., Bäck, S., Engelholm, S. and Engström, P., 2020. Surface-guided tomotherapy improves positioning and reduces treatment time: A retrospective analysis of 16 835 treatment fractions. Journal of Applied Clinical Medical Physics, 21(8), pp.139-148.

[15] Haraldsson, A., Engleson, J., Bäck, S., Engelholm, S. and Engström, P., 2019. A Helical tomotherapy as a robust low-dose treatment alternative for total skin irradiation. Journal of Applied Clinical Medical Physics, 20(5), pp.44-54.

[16] Kügele, M., 2021. Surface guided radiotherapy.

[17] Oh, S. and Kim, S., 2017. Deformable image registration in radiation therapy. Radiation Oncology Journal, 35(2), pp.101-111.

[18] Pallotta, S., Kugele, M., Redapi, L. and Ceberg, S., 2020. Validation of a commercial deformable image registration for surface-guided radiotherapy using an ad hoc-developed deformable phantom. Medical Physics, 47(12), pp.6310-6318.

[19] Kügele, M., Mannerberg, A., Nørring Bekke, S., Alkner, S., Berg, L., Mahmood, F., Thornberg, C., Edvardsson, A., Bäck, S., Behrens, C. and Ceberg, S., 2019. Surface guided radiotherapy (SGRT) improves breast cancer patient setup accuracy. Journal of Applied Clinical Medical Physics, 20(9), pp.61-68.

[20] Mannerberg, A., Kügele, M., Hamid, S., Edvardsson, A., Petersson, K., Gunnlaugsson, A., Bäck, S., Engelholm, S. and Ceberg, S., 2021. Faster and more accurate patient positioning with surface guided radiotherapy for ultra-hypofractionated prostate cancer patients. Technical Innovations Patient Support in Radiation Oncology, 19, pp.41-45.

[21] Lempart, M., Kügele, M., Ambolt, L., Blad, B. and Nordström, F., 2016. Latency Characterization of Gated Radiotherapy Treatment Beams Using a PIN Diode Circuit. IRBM, 37(3), pp.144-151.

[22] Al-Hallaq, H., Cerviño, L., Gutierrez, A., Havnen-Smith, A., Higgins, S., Kügele, M., Padilla, L., Pawlicki, T., Remmes, N., Smith, K., Tang, X. and Tomé, W., 2022. AAPM task group report 302: Surface-guided radiotherapy. Medical Physics,.

[23] Haraldsson, A., Engellau, J., Lenhoff, S., Engelholm, S., Bäck, S. and Engström, P., 2019. Implementing safe and robust Total Marrow Irradiation using Helical Tomotherapy – A practical guide. Physica Medica, 60, pp.162-167.

[24] Khan F.M. The Physics of Radiation Therapy. Lippincott Williams Wilkins; Philadelphia, PA, USA: 2003. pp. 429–430.

[25] Metodbeskrivning TMI, Engström, P., Engellau, J., Löfgren, A., Byrén, C., 2017. Total Marrow Irradiation (TMI) med Tomoterapiteknik, Skånes universitetssjukhus, VO Hematologi, Onkologi och Strålningsfysik.

[26] van Herk, M., Remeijer, P., Rasch, C. and Lebesque, J., 2000. The probability of correct target dosage: dose-population histograms for deriving treatment margins in radiotherapy. International Journal of Radiation Oncology*Biology*Physics, 47(4), pp.1121-1135.

[27] Rasch, C., Barillot, I., Remeijer, P., Touw, A., van Herk, M. and Lebesque, J., 1999. Definition of the prostate in CT and MRI: a multi-observer study. International Journal of Radiation Oncology*Biology*Physics, 43(1), pp.57-66.

[28] Remeijer, P., Rasch, C., Lebesque, J. and van Herk, M., 1999. A general methodology for three-dimensional analysis of variation in target volume delineation. Medical Physics, 26(6), pp.931-940.

[29] Corrao, G., Rojas, D., Ciardo, D., Fanetti, G., Dicuonzo, S., Mantovani, M., Gerardi, M., Dell'Acqua, V., Morra, A., Fodor, C., Galimberti, V., Veronesi, P., Cattani, F., Orecchia, R., Jereczek-Fossa, B. and Leonardi, M., 2019. Intra- and inter-observer variability in breast tumour bed contouring and the controversial role of surgical clips. Medical Oncology, 36(6).

[30] Makrogiannis, S., Boukari, F. and Ferrucci, L., 2018. Automated skeletal tissue quantification in the lower leg using peripheral quantitative computed tomography. Physiological Measurement, 39(3), p.035011.

[31] Conson, M., Cella, L., Pacelli, R., Comerci, M., Liuzzi, R., Salvatore, M. and Quarantelli, M., 2014. Automated delineation of brain structures in patients undergoing radiotherapy for primary brain tumors: From atlas to dose–volume histograms. Radiotherapy and Oncology, 112(3), pp.326-331.

[32] Ecclestone, G., Bissonnette, J. and Heath, E., 2013. Experimental validation of the van Herk margin formula for lung radiation therapy. Medical Physics, 40(11), p.111721.

[33] Groher, M., Kopp, P., Drerup, M., Deutschmann, H., Sedlmayer, F. and Wolf, F., 2017. An IGRT margin concept for pelvic lymph nodes in high-risk prostate cancer. Strahlentherapie und Onkologie, 193(9), pp.750-755.

[34] de Boer, H. and Heijmen, B., 2001. A protocol for the reduction of systematic patient setup errors with minimal portal imaging workload. International Journal of Radiation Oncology*Biology*Physics, 50(5), pp.1350-1365.

[35] Gordon, J. and Siebers, J., 2007. Convolution method and CTV-to-PTV margins for finite fractions and small systematic errors. Physics in Medicine and Biology, 52(7), pp.1967-1990.

[36] Herschtal, A., Foroudi, F., Silva, L., Gill, S. and Kron, T., 2012. Calculating geometrical margins for hypofractionated radiotherapy. Physics in Medicine and Biology, 58(2), pp.319-333.

[37] Radixact® Treatment Delivery System-Physics Essentials Guide Version 3.0.x, Accuray Incorporated, Wisconsin 53717 USA, Date of Revision: 2021-05.

[38] Hui, S., Lusczek, E., DeFor, T., Dusenbery, K. and Levitt, S., 2012. Three-dimensional patient setup errors at different treatment sites measured by the Tomotherapy megavoltage CT. Strahlentherapie und Onkologie, 188(4), pp.346-352.

[39] Svahn-Tapper G, Nilsson P, Jönsson C, Alvegård TA. Calculation and measurements of absorbed dose in total body irradiation. Acta Oncol. 1990;29:627-633. https://doi.org/10.3109/0284186900 9090064

8 Appendix

8.1 Clinical practice - Kyoto Phantom

The surface of the Kyoto phantom and is presented along with the suggested deviations (Figure 15). The reference surface is blue and the live surface green. As seen in the figure, most parts of the surfaces are aligned but a deviation is seen on the shoulder. The deviation of the shoulder was noted but not possible to correct for.

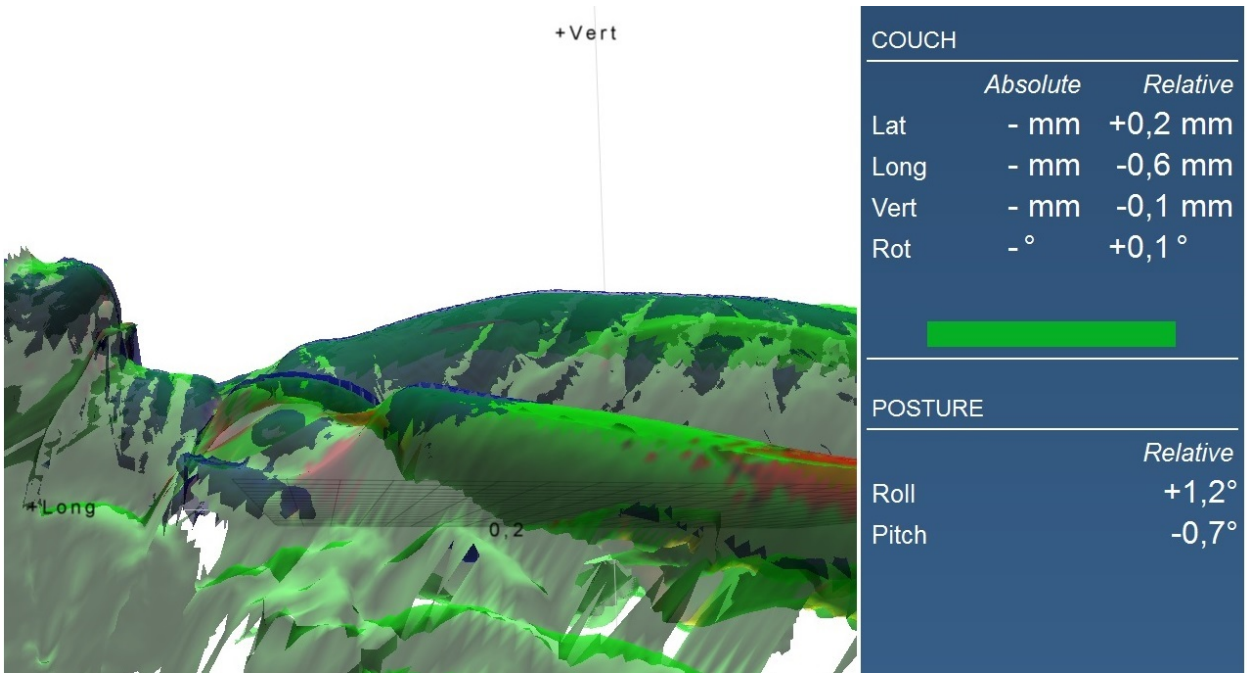

Figure 15: *Kyoto phantom being positioned with the OSS system. Deviation seen on the shoulder between live and reference surface.*

The kVCT scan of the phantom is presented along with the positioning errors after automatically matching with the reference CT (Figure 16). The deviation of the shoulder is also seen in the image.

Figure 16: *kVCT image registration of Kyoto phantom after being positioned with the OSS system.*